1. Introduction

Maritime stratus clouds are of utmost importance to global climate because of their large extent, large contrast in cloud versus surface albedo, and susceptibility to anthropogenic influence. Manmade particles due to air pollution produce both the 1st and 2nd indirect aerosol effects (IAE) by increasing cloud droplet concentrations, which increase cloud albedo and cloud extent respectively. Both of these IAE processes increase planetary albedo. Since IAE is the largest climate uncertainty [*IPCC,* 2007], measurements of the aerosol that affects these clouds is of interest.

These measurements were made as part of the 2005 Marine Stratus Experiment (MASE), which is described by *Ghan and Schwartz* [2007]. The Battelle G1 aircraft made a total of 13 flights. The first on July 5 was a test flight. The second also brief flight of July 6 was the only flight in clean maritime air. The third flight on July 12 was the only late afternoon flight and the only cloud-free flight. All of the other flights took place between 1000 and 1400 local Pacific daylight time (PDT). The flight of 23 July was in broken stratus. The rest of the flights July 15, 16, 17, 18, 19, 20, 22, 25, and 27 took place with mostly solid stratus decks. The CCN instruments did not operate properly on the last flight—July 27—and ambient data were limited on the 2nd from last flight because size-critical supersaturation (S_c) measurements occupied much of the time for one of the instruments [*Hudson*, 2007]. Thus this analysis covers 11 flights exclusive of only the first (July 5) and last flights (July 27). Eight of these flights were in extensive low polluted stratus.

Each flight began and ended with a descent and ascent, respectively at Pt. Reyes on the coast 80 km north of San Francisco. Then the aircraft proceeded to locations much further from shore where concentrations were consistently and significantly lower. In an effort to report measurements more representative of greater areas, this analysis is focused on the mid-flight measurements (usually between 1100 and 1300 PDT) made 80-190 km to the west of Pt. Reyes on July 6, 12, 19, 20, 22, 23, and 25 and 160 km to the south-southeast of Pt. Reyes approximately 30-60 km southwest of Monterey Bay for July 15, 16, 17, and 18.

2. Instruments

CN were measured with a TSI 3010, which has a lower size threshold of 10 nm where the efficiency should be 50%. This instrument operates continuously and the particles are counted individually. The pulses caused by condensed alcohol on each particle are integrated over specific time intervals that were usually 1s in length.

The DRI CCN spectrometers deduce spectra simultaneously from the sizes that droplets attain within a continuous flow thermal gradient diffusion cloud chamber. These chambers are actually six (new spectrometer) or eight (old spectrometer) chambers in series with carefully controlled temperatures on each set of plates, internal pressure and flowrates [*Hudson*, 1989]. The lower S_c nuclei (better CCN) produce larger cloud droplets. The droplets are counted and sized individually as they pass through an optical particle counter immediately upon exiting the cloud chamber. These instruments must be calibrated with particles of known S_c in order to relate droplet size (actually the channel number of a pulse height analyzer) to S_c. This is done with NaCl aerosol that has passed through a differential mobility analyzer (DMA) at various size settings that are produced by using different voltages. The narrow size distribution from the DMA produces a narrower droplet size distribution in the cloud chamber than the droplet size distributions of ambient aerosol. The subsequent plot of the mean channel number of each distribution against the theoretical S_c of the DMA-sized NaCl is then used to relate channel

number (i.e., cloud chamber relative droplet size) to S_c so that a spectrum can then be deduced when ambient aerosol is sampled [*Yum and Hudson*, 2001]. An earlier version of the present DRI CCN spectrometers that used the same principles of operation agreed with the best CCN instruments tested in the last international CCN workshop [*Hudson and Alofs*, 1981; *Kocmond et al.*, 1981]. The DRI instruments also agreed with size-resolved hygroscopicity predictions of CCN [*Gasparini et al.,* 2006].

There is some uncertainty in ambient spectral measurements due to artificial instrument broadening, coincident pulses and vapor depletion. The broadening error mainly affects the wings of the distribution but has little effect on the peak or the mean. Broadening causes greater errors for steep distributions, i.e., greater real differences in concentrations as a function of S_c (channel number) that are erroneously reduced. Coincidence and vapor depletion errors increase with concentration and can thus be mitigated by using smaller sample flows, but this can result in greater diffusion losses, which are greater for smaller (usually higher S_c) particles. Coincidence generally falsely converts two high S_c (small cloud chamber droplets) to one low S_c (large apparent cloud chamber drops). The latter is the greater error (overestimate) because of the typically lower concentrations of the low S_c particles. Vapor depletion on the other hand generally shifts all aspects of the spectra to higher S due to the reductions of droplet size due to the reduction of cloud chamber S due to greater competition for water vapor.

These CCN spectrometers produce simultaneous measurements of CCN spectra [e.g., *Hudson and Xie*, 1999; *Yum and Hudson*, 2001] over a large S range. Measurements below 0.1% S are a unique feature of the DRI CCN spectrometers that is especially important for the lower cloud supersaturations that are expected for both stratus or polluted clouds. These measurements were of utmost importance to the MASE clouds because they were both stratus and polluted. In recent projects such as MASE two DRI CCN spectrometers have made simultaneous measurements over different but overlapping S ranges. Since the lower part of the S range of an instrument is more challenging, the upper S part of the range of an instrument operating over a lower S range (e.g., 0.01-0.5%) can be used to check the performance of the lower S portion of another instrument operating at a higher and greater S range (e.g., 0.02-2%). If there is agreement between these instruments in an overlapping range this tends to verify the accuracy of the higher range instrument at least within that overlap band. But this also tends to confirm the higher S measurements because the instrument is less challenged at higher S.

3. Measurements

A low turbulence inlet operating at nearly isokinetic flow was used to get sample into the aircraft where it was tapped by another tube to take sample into the CN and CCN instruments similar to previous arrangements on other aircraft [e.g., *Hudson and Frisbie,* 1991; *Hudson and Xie,* 1999; *Yum and Hudson*, 2001]. This inlet should pass particles smaller than 1.5 µm with 50% efficiency according to fluid dynamics calculations. However, as was the case in previous projects cloud droplets are usually too large to adequately sample with such an inlet. This leads to two major reasons that valid CN and CCN measurements within clouds are not possible. First many CCN are within some of the cloud droplets that are too large to pass through the sample inlet. Since it is usually difficult to determine how many droplets are lost in the inlet, the in-cloud CN and CCN measurements are thus rather indeterminate. If all activated droplets were lost then only the interstitial CCN would be measured but this is usually not the case. Moreover, there is often difficulty separating activated cloud droplets from unactivated haze droplets, especially in polluted clouds where the activated cloud droplet sizes are limited by competition.

Because competition also limits the cloud supersaturation (S) this means that lower S_c particles remain as unactivated haze droplets with consequent larger sizes that are often similar to the activated cloud droplet sizes, hence the confusion. Second the cloud droplets are often large enough to splash the inlet and thus produce false high counts of fragments that usually appear to be small (high S_c) particles. For these two reasons the measurements that took place within clouds were discarded from this analysis. This severely limited the low altitude data because most of the clouds encountered during MASE were very low and often extended to or very close to the ocean surface or at least down to the lowest flight altitude (~ 100m).

High and variable CN concentrations due to inlet splashing are usually good indicators of the presence of cloud. Therefore, this indication and the Gerber PVM probe liquid water measurements usually provided enough information to correctly remove cloudy periods from the CCN data sets. Nonetheless, this was a tricky exercise that may not have always worked. However, there were also many periods when the airplane was definitely below cloud base and thus not perturbed by the clouds. The below cloud measurements are very important because they are generally thought to represent the CCN that the cloud droplets condense upon. However, stratus clouds are also subject to an indeterminate amount of entrainment. Since they usually have considerable horizontal extents, as was certainly the case during MASE, this means that the only source of entrained air was from above the clouds. Therefore, the air immediately adjacent to cloud top may also be relevant to stratus cloud microphysics. Since there were usually significant differences between the below and above cloud concentrations it is worthwhile to characterize both of these sets of measurements. Therefore, the data were partitioned according to altitude intervals. This analysis focuses on the two narrow layers; 1) between cloud base and the lowest flight altitude (100m), and 2) within 10 mb pressure altitude of cloud top.

The major feature of these MASE particle measurements was the concentration differences as a function of altitude. Figure 1 shows an example of one of the complete soundings that was done at the end of the July 16 flight. This near-shore sounding is displayed because there were no such long soundings out over the ocean and for this flight the concentrations at Pt. Reyes happened to be similar at all altitudes and CCN S to the concentrations measured during the middle of this flight much further from shore. This flight was exceptional in this respect because most of the time the concentrations near Pt. Reyes were significantly higher than they were further out over the ocean. In order to display the vertical differences in concentrations out over the ocean it was necessary to piece together various measurements obtained during the various horizontal flight legs and vertical soundings by taking average concentrations within 10 mb pressure altitude ranges. This is shown in Figure 2 for the 9 flights with polluted stratus (July 15-25). These altitude bins have been normalized to the altitude of cloud top on each flight, which was rather consistent throughout the middle parts of each flight. Since it is not possible to obtain valid CN or CCN measurements within cloud and since these cloud bases were usually so low that it was often difficult to obtain below cloud measurements, all below cloud measurements are lumped together and arbitrarily set at –25mb in Fig. 2. Cloud depths ranged from 100-400 m.

The concentrations closest to the clouds below and above are the focus of this research since they are the most likely to influence cloud microphysics and since they were so often quite different. The differences in particle concentrations between below and just above cloud top were weakly related to the average temperature difference between these two levels—correlation coefficient 0.60, which is significant to 5% for these 9 data points. These strong temperature

inversions (8-17C average 12C) that are typically associated with stratus cloud systems, especially over the ocean, are probably a major reason for the vertical structure of the particle concentrations. The affect of the clouds (aerosol scavenging) confined as they are below the stable layers, is also a factor in the observed vertical concentration differences. Tables 1 and 2 show the average concentrations below and just above these clouds for all flights. Table 3 displays the flight-averaged ratios of the above to below cloud concentrations that are also seen in the lowest two levels displayed in Fig. 2 for CN and CCN @ 1% S and 0.1% S. Table 4 shows the relative standard deviations (sd)--sd/mean--of the below cloud measurements. This was similar for the above cloud measurements.

Figure 2 shows that there were usually layers of aerosol above the clouds that were higher in concentration than the below cloud measurements. Table 3 and Fig. 2 show that this usually resulted in higher concentrations immediately above cloud compared to below cloud. The most notable exception was July 23, which was in broken somewhat higher cloud. On this flight there was a layer of higher concentrations well above the clouds. July 22 is another exception where the concentrations just above are similar to the below cloud concentrations, but there is again a higher concentration layer further up. July 17 is an exception only for CN, but this is mainly due to the exceptionally high below cloud CN concentration (by far the highest of the nine flights). Figure 3 shows average CCN spectra above and below cloud for the eight flights with unbroken polluted stratus decks. Figure 4 shows the average above and below cloud spectra of these eight flights and the one flight that had marine concentrations.

4. Data

MASE CCN data was put into the archive in early 2007. For almost all of the time throughout all of the flights concentrations at 10 different S with time intervals of a few seconds were put into the archives. These S values were 1, 0.6, 0.4, 0.3, 0.2, 0.1, 0.08, 0.06, 0.04, and 0.02%. Exceptions were: July 15 no 0.4% S data; July 18 no 0.4 and 0.3% S data from 1238-1304 PDT; July 22 no data for S < 0.1% from 1012-1135 and 1231-1313; July 23 no 1% S data; July 25 there were gaps for 1, 0.6, and 0.4% S because of size-S_c measurements; July 27 there was 1 and 0.6% S data for only 927-1001. Additional S values were reported for: July 12 0.5% S; July 15 0.15% S; and July 25 0.15% S. As per preferences expressed by some science team members the data obtained within clouds were not removed. However these data have limitations due to inlet splashing and the fact that an unknown number of particles may not have been sampled due to the fact that they were within cloud droplets that may or may not have been sampled. Science team members would have to make their own decisions about these data.

5. Trajectory Analyses

The July 6 flight showed concentrations characteristic of clean maritime air but all of the other flights displayed considerably higher concentrations that suggest continental and anthropogenic influence. With the exception of the clear air (July 12), broken stratus (July 23) and July 22 flight the concentrations were even higher above than below the clouds (Tables 2 and 3) except for some of the low S measurements (i.e., July 15, 18, 20 and 25).

Trajectory analyses with the NOAA HYSPLIT program often showed different back trajectories for the below and above cloud air parcels. For July 6 there were similar below and above cloud back trajectories—north-northwest parallel to the coast for the previous 24 hours that bent at the California-Oregon border to west-southwest for the previous 3 days. This is consistent with the lowest concentrations observed on this flight. Trajectories for July 12 were

similar except that they bent more to straight west and there were greater differences in the above and below cloud trajectories. Although the low altitude concentrations are considerably higher than July 6 the higher level concentrations though higher than July 6 are considerably lower than the low altitude concentrations and the high altitude concentrations of subsequent flights. Trajectories of July 15 show a good deal of local meandering with differences above and below cloud. It is only beyond 3 days that the back trajectories bend to the west. This is consist with the higher concentrations compared to the previous flights, but lower concentrations than subsequent flights. July 16 shows considerable differences in the above/below trajectories with the low altitudes running north-northwest parallel to the coast and the above cloud trajectories displaying meandering and southerly flow. There is also a considerable contrast in the altitudes of origin for the above and below trajectories. These differences in trajectories seem to be in keeping with the differences in the below versus above concentrations and the highest above cloud concentrations for this flight.

The July 17 trajectories and CN and high S CCN concentrations are similar, but the back trajectories were more meandering at the low altitudes and there were more southerly origins for the above cloud trajectories. This difference may be the reason for the large differences in concentrations at lower S. The July 18 trajectories are nearly identical below and above cloud, which is consistent with the lowest above/below ratio except for the broken stratus flight of July 23 and the July 22 flight. However, the unwavering northerly flow belies the high concentrations that were observed on July18. July 19 shows more meanderings and sharper differences in the above versus below trajectories with an ultimate (3 or 4 days) southerly origin above and northerly origin below. This may be consistent with the 2nd greatest overall difference in above/below concentrations. July 20 shows a sharp above/below contrast in that the below origin is north and the above origin is from the south. This is consistent with the 4th greatest below/above concentration contrast. The July 22 trajectories show considerable meandering. July 23 shows the only definite continental origins. This or the lack of clouds may be responsible for the highest concentrations of low S CCN. July 25 shows unwavering northerly trajectories and a return to somewhat lower concentrations especially for the lower S particles.

6. Instrument Comparisons

Figure 5 shows simultaneous measurements with the two DRI CCN spectrometers. The panels on the left show measurements that were made at very low altitudes below the low stratus clouds. The panels in the right hand columns display the corresponding just-above-cloud-top (within 10 mb pressure altitudes of cloud top) concentrations for that flight. The old instrument operated at lower delta T values that produced a smaller (lower) range of S. The lower limit ranged from 0.01-0.02% and the upper limit ranged from 0.1-0.5%. The new instrument operated at S up to 2%. Its lower limit of validity varied from 0.1-0.01% S. The measurements shown in Fig. 5 were all of the below and just above cloud time periods out over the ocean away from Pt. Reyes during each flight when there were simultaneous valid ambient measurements with both instruments. Excluded are the time periods when the aircraft was within clouds, when one instrument was being calibrated, or making volatility or size-S_c measurements or otherwise not obtaining valid ambient spectra. The new instrument usually operated at 1 s time intervals while the old instrument generally operated at 3s intervals. The total periods of simultaneous measurements were made up of 1 to 32 disjoint periods of various consecutive times ranging from 3 to 900s. In each panel of Fig. 5 are shown the total number of seconds of simultaneous data, which is also shown in Table 5 columns 1 and 6. Also in each Fig. 5 panel is the time

period over which these measurements were obtained rounded to the nearest minute, and the percentage of time out of this total length of time for which there were valid simultaneous measurements (the dividend of the number of seconds and minutes that is displayed in each panel). All of these numbers varied considerably among the flights depending mainly on the altitude track of the airplane and cloudiness. They generally do not reflect instrument deficiencies but rather the degree of cloudiness or the differences in flight paths of the airplane.

There are four times as many below cloud as above cloud simultaneous measurements as shown at the bottom of columns 1 and 6 of Table 5--5971 versus 1431 total seconds. The five shortest simultaneous times (see also Table 5 columns 1 and 6) are above cloud and the seven longest simultaneous measurements are below cloud. So the greater statistics of most of the below cloud measurements generally provided better agreement between instruments. Shorter intervals are also subject to more edge errors due to slightly different measurement periods of the two instruments (fractions of seconds) when concentrations are changing. Most of the worst agreements were for short measurement periods; i.e., the shortest Fig. 5f (July 15 above, 20s), and 4^{th}-6^{th} shortest Figs. 5v, 5l, and 5u at 46, 52, and 88s respectively. Only the last of these was below cloud. Those with longer periods tended to show better agreement, notably the longest period (Fig. 5k, July 18 below, 1236s), the 4^{th}-6^{th} and 8^{th} longest Fig. 5s, 5a, 5q, and 5b with 735, 559, 497, and 364s respectively. Only the last of which was above cloud. Agreement was excellent at all S for 3j and 3t even though agreement is not expected at low S where new should be most inaccurate; i.e., Fig. 5c, 5e, 5g, 5m, 5n, 5r, and 5w show excellent agreement except at low S. The others Fig. 5d, 5h, 5i, 5o, 5p, and 5x at the least display good agreement in the 0.1-0.2% overlapping S range.

Figure 6 shows the Fig. 5 data plotted in the traditional cumulative fashion. The red lines are for the new spectrometer and the green lines are the composites of the two instruments. Below an S where the instruments show good agreement in Fig. 5 the green line is the old spectrometer data. Above that S the data from the new spectrometer is incrementally added to continue the green lines. Both of these lines are only for periods when there was simultaneous data from both instruments. Since the green line should be more accurate, comparisons of these two lines demonstrates that the inadequacy of the larger range instrument at low S can sometimes extend into its valid S range when cumulative concentrations are considered. Nevertheless, the errors have limited propagation to higher S because they are a smaller percentage of the higher S concentrations because of the relatively low concentrations of low S CCN.

For the most part the cumulative agreements in Fig. 6 appear to be similar to the corresponding panels in Fig. 5. The short measurement times that showed more disagreements in Fig. 5 (f, v, l, and u) are again among the worst. But here 6r, which is after all the third shortest period, also shows relatively poor agreement whereas it showed good agreement at least at high S in Fig. 5. Figs. 6k, q, and b continue to show the same excellent agreements that they showed in Fig. 5, but Fig. 6s and a are not so good although the disagreements at low S in Fig. 3 reveal the reasons. Fig. 6j shows the same excellent agreement as in Fig. 5j except at S below 0.04%. However Fig. 6t shows limitations there that were not as apparent in Fig. 5t, but this was after all the 2^{nd} shortest measurement. Figs. 6c, e, m, and n show good agreement at all but the lowest S just as they did in Fig. 5. But Fig. 6g, r, and w propagate the low S errors shown in Fig. 5. July 22 above (Fig. 6r) was the third shortest. Figs. 6d, h, i, and p show similar agreements to Fig. 5 but Figs. 6o and x seem to have compensating errors that make them appear better than they did in Fig. 5. Comparisons between Figures 5 and 6 demonstrate the superiority of the more

rigorous differential spectral comparisons and the limitations of cumulative comparisons of CCN instruments that operate over different S ranges. The differential spectra (Fig. 5) are also better indicators of the variability of the CCN spectra than cumulative spectra (Fig. 6), which tend to blur contrasts. The differential spectra are also better indicators of the relative differences in concentrations over the different S. The fact that the agreement between instruments holds over wide ranges of concentrations and spectral shapes also tends to verify the accuracy of the measurements.

Also shown in Figure 6 is the total average cumulative concentrations of the new instrument for all valid ambient measurements during the given flight altitude ranges for the middle parts of the flights. Comparisons of these symbols with the red lines show the possible bias of considering only the data that is simultaneous with the old spectrometer. Figs. 6a-f, h-k, n, o, and q indicate that there was little non-simultaneous new spectrometer data or that the non-simultaneous data for these 12 sets was similar to the simultaneous data. Indeed these periods are identical for d-July 12 above, k-July 18 below and o-July 20 below as shown in columns 1-3 and 6-8 of Table 5. The other 9 of these panels with good agreement have an average ratio of simultaneous to total new periods of 0.56 with a range of 0.22-0.70. Panels s, u, w, and x should not show such similarities because the simultaneous below cloud data was divided into high and low concentration periods whereas the total concentrations (symbols) are the average over both sets of periods. The main reason for the discrepancies for the other seven panels 4g, l, m, p, r, t, and v is that the simultaneous-to-total new data periods average only 0.22 with a range of 0.11-0.32.

The comparisons in Fig. 5 reveal the precision that also attests to the accuracy of these measurements. The comparisons in Fig. 6 also indicate this and they demonstrate something about the variability and representativeness of measurements over different or limited time periods.

7. Variability

The error bars in Fig. 6 indicate the standard deviations of the new spectrometer measurements. This cannot be computed for the combined data, but this should be a reasonable estimate of the overall variability of the concentrations. There is only a slight anticorrelation between the total length of time of the simultaneous measurements and the standard deviation. Table 4 shows the relative sd (sd/mean) of the cumulative concentrations for the below cloud data shown in Fig. 6. This was similar for above cloud measurements. The CN and CCN relative sds are not readily comparable because they often did not span the same time periods mainly because the CN instrument was sometimes otherwise occupied, mainly calibrating the older spectrometer. Nevertheless, the CN and CCN sds were usually comparable with each other. The only exception was July 12 when the CN counter measured for less than 2 minutes. Often the CN concentrations varied significantly more than the CCN indicating that the smaller particle concentrations varied more.

These considerable sds are based on data records that were each integrations of individual pulses over 1s time intervals. Since the CN sample flow rate was 16.67 cm^3/sec (1 liter/minute) of which all particles were counted, this meant that the number of counts in each record was 16.67 times the displayed mean concentration. Thus for an average concentration of 1000 cm^{-3} approximately 16,667 pulses were individually counted in each 1 second integration record. Thus if the actual concentration remained constant, the sd should be approximately the square root of the average number of counts in each record, 129, which is 0.77% of the mean. The CCN

spectrometers had much lower flowrates of approximately 0.33 cm^3/s. Since this is a factor of 50 lower than the CN flowrate the statistical sd of the CCN instruments should be a factor of 7 greater than the CN instrument, i.e., 5.4% for 1000 cm^{-3} with steady concentrations. Table 4 shows that the actual variability of each flight greatly exceeded these values and was thus real and not caused by the limitations of the instruments to detect variability. The fact that the relative variability was usually similar in the two instruments suggests the reality of the variability, which is further illustrated by the example in Fig. 7a. On the other hand there were some periods when the concentrations were steady. Although these were less than 90s in length (most less than 15s) they represent more than a km of distance since the airplane was traveling at 100 m/s. During some of these periods the measured relative sds were comparable to the relative square roots of the total number of particles counted in each record (Table 6). Under these conditions CN standard deviations were only 1% of the mean concentrations (Fig. 7b). Since this is the limit of variability detection of this instrument, the actual consistency may have been even better. Although the CCN standard deviations were higher they were also comparable to the limit of variability detection of the CCN instrument. Since the CCN and CN concentrations were similar the actual variations were probably also similar to the lower values reported by the CN instrument. These observations suggest that there are reasonably large scales over which input particle concentrations are quite unvarying. Therefore, clouds formed in such air masses that display greater variations in droplet concentrations must be due to reasons other than variations in CCN concentrations; i.e., dynamic processes.

8. Comparisons with Previous Data.

Hudson and Frisbie [1991] and *Hudson and Xie* [1999] reported aerosol layers above marine stratus off the southern California coast. Although there are greater pollution sources in southern California the concentrations were much lower in that 1992 study than those reported here off the central California coast at virtually the same time of year and with the same types of clouds and with the same instruments. Overall average concentrations in Table 1 ranged between a factor of 2 to a factor of 5 progressively higher from 0.04 to 1% S compared to row 1, Table 3 of *Hudson and Xie* [1999]. One reason may be the greater distances from the coast in four of the five flights of the earlier measurements. Only the July 6 flight had concentrations similar to the 1992 FIRE project. The July 6, 2005 concentrations ranged from 25% higher at 1% S to approximately equal at 0.3% S and 65% lower (one-third) at 0.04% S than the average of the 1992 southern California measurements [*Hudson and Xie*, 1999].

These MASE concentrations were intermediate to the maritime and continental concentrations reported in the eastern Atlantic (ASTEX) by *Hudson and Xie* [1999]. The overall averages here are a factor of two (at 0.04% S) to a factor of 3 (at 1% S) higher than the average eastern Atlantic maritime concentrations in that same table of *Hudson and Xie* [1999]. They are a factor of 3 to 2 (going from low to high S) lower than the eastern Atlantic continental concentrations. The lowest flight-averaged concentrations (July 15, 16, 20, and 22) were still generally a factor of two higher than the eastern Atlantic maritime. The only exception to this was the low S measurements of July 15, which were comparable to the ASTEX average maritime concentrations.

Hudson et al. [2000] reported CCN measurements off the central California coast in the same area as some of these measurements (off Monterey) also below low stratus clouds in late June, 1994. Figure 1a of that article shows "dirty background concentrations" that were approximately half of the averages found in this study—60% at 1% S, 50% at 0.1% S and 40% at

0.04% S. However, the July 15 flight averages closely match those 1994 measurements, both of which were made off Monterey.
The maritime measurements of *Hudson and Xie* [1999] were comparable to previous maritime CN and CCN measurements by other investigators [i.e., *Twomey and Wojcieshowski*, 1969]. Comparisons with the present study strongly indicate that the MASE 2005 measurements were not at all characteristic of maritime air masses except for the July 6 flight. Therefore, the boundary layer concentrations here are most certainly affected by continental and probably anthropogenic sources. Thus the higher concentrations above the clouds were most likely of anthropogenic origin.

9. Aerosol Processing

During the last half of the project volatility measurements were also made. This is done by passing the sample through an oven that heats it to various temperatures up to a few hundred degrees. This is accomplished by turning a valve to periodically divert the sample for periods of one or two minutes through a tube that passes through the oven. The comparisons of these measurements with the interspersed ambient measurements (back and forth every minute or two) determines the loss of particles due to heating. Comparisons can also be made with the other CCN instrument that continued to monitor the ambient air directly. Various compounds disappear at various temperatures so that the particle concentrations are often lower upon heating. Heating can also reduce particle sizes, which is reflected in a shift of the CCN spectrum. Over the course of several minutes the oven temperature was often changed to obtain volatility measurements at a range of temperatures. Volatility is excellent for determining the presence of NaCl because it does not volatilize until about 600 degrees C. On the other hand the more common atmospheric CCN component, sulfate, volatilizes at only 200 degrees C. There were significant differences in the CN and CCN volatility measurements that provide clues about the mixing state of the aerosol. Namely that relatively higher heated CN concentrations compared to CCN concentrations suggests an internal mixture of soluble and insoluble or less water-soluble components.

Volatility measurements made on the 20th, 22nd, 23rd, and 25th shown in Figs. 8, 9, and 10 indicate that most CCN (~90% though some variability) behave like ammonium sulfate in that they volatilize at approximately 200 degrees C. Most of the CN measurements indicated higher volatility temperatures for most of those particles but the CN volatility measurements showed much more variability. The volatility measurements in MASE are consistent with volatility measurements in other projects [*Hudson and Da*, 1996]. These volatility measurements are also consistent with the size-critical S (S_c) measurements in that many of the particles appear to be internally mixed soluble volatile material (i.e., ammonium sulfate) with insoluble nonvolatile material (e.g., carbon).

During the last successful CCN flight on July 25 another sample processing technique was done--measurement of CCN size. This is done by passing the sample through the same DMA that is used for calibrations. The difference is that instead of particles of known composition from the aerosol generator, the ambient outside sample is passed through the DMA. The DMA passes only particles within a limited size range that is then sent to one of the CCN spectrometers. This allows a determination of the critical S (S_c) of only particles within a small size range. When several different sizes are used by changing the voltage of the DMA over a period of several minutes a relationship can be obtained between dry particle sizes and S_c. This can then be compared with theoretical relationships for various substances such as NaCl and

ammonium sulfate. *Hudson and Da* [1996] found that in clean maritime air CCN particle sizes were characteristic of highly soluble compounds such as NaCl or ammonium sulfate. In more continental or polluted air, which is usually characterized by higher particle concentrations, the size-S_c relationship is quite different. The data falls further from the theoretical relationships for NaCl and ammonium sulfate, which indicates that the particles are less soluble or that they are internally mixed with insoluble material. This seems to be consistent with the fact that carbon based compounds, which are not very soluble are more common in polluted air masses. Figures 11 and 12 show that the air above the clouds, which usually displayed higher particle concentrations, was even less soluble than the somewhat cleaner air below the clouds. Figure 11 shows that the sizes of these particles are larger than they are for ammonium sulfate or NaCl of the same critical supersaturation (S_c). In other words it takes more of this ambient aerosol to make the same solubility as the purer soluble materials shown. This is because the material is less soluble or that the soluble material is internally mixed with insoluble material that adds to the size but not to the nucleating ability of the particle. Figure 12 shows the hygroscopicity (B) which is lower for less soluble material. The B values in MASE correspond to B values obtained in other polluted air masses.

Dusek et al. [2006] challenged the value of atmospheric chemistry with regard to the indirect aerosol effect by maintaining that particle size measurements might be sufficient to determine CCN. However, that assertion was based on the rather limited variability of the size-S_c relationships that they measured in Germany. The limited range that they measured is inconsistent with *Hudson and Da* [1996] and *Hudson* [2007], which includes Figure 11 .

10. Conclusions

Persistent high CN and CCN concentrations characteristic of continental/anthropogenic air masses were consistently measured at distances up to 200 km from the central California coast over a 10-day period. These measurements were made in association with widespread stratus cloud systems where concentrations were up to a factor of two higher above than below the clouds. Higher concentrations above clouds that were also consistently observed by *Hudson et al.* [1998] and *Yum and Hudson* [2001] were attributed to cloud scavenging. The relatively lower below cloud concentrations observed here are probably also a result of cloud scavenging. Although cloud droplet concentrations are generally thought to be established at the base and thus related mainly to cloud base CCN, entrainment of air from above clouds also affects cloud microphysics. The fact that this air often contains significantly different CCN concentrations is important to efforts to understand these clouds and how they are disposed to the indirect aerosol effect.

Extensive comparisons were made between two similar CCN spectrometers that operated at different supersaturation (S) ranges. Agreement between these instruments within the S overlap range centered at 0.1% for a variety of concentrations and spectral shapes indicates the precision and suggests accuracy of these difficult CCN spectral measurements. The comparisons were better when averaged over longer time intervals probably because the edge inconsistencies were overwhelmed. Comparisons of data obtained over somewhat different time spans also yielded information about the variability of the concentrations and the ability to detect representative concentrations with various measurement periods. Comparisons of differential and cumulative spectral presentations showed the superiority of more rigorous differential plots and some of the limitations of traditional cumulative plots.

Average concentration variations among the 8 or 9 flights with polluted stratus were a factor of two. Variability in high S CCN concentrations out over the ocean during the 2 hours of mid-flight measurements ranged between 15 and 56% in relative standard deviation for each of the flights. However, there were shorter periods that covered 1-9 km when the concentrations varied by less than 1%. This could have important implications for understanding cloud microphysics, which will be the subject of a subsequent article on the MASE clouds [*Daum et al.,* 2008].

Volatility and size-S_c measurements in MASE were consistent with measurements in polluted air masses in several previous measurement programs. The higher concentrations above the clouds appeared to be even more polluted because they were more insoluble than the particles below cloud.

References

Daum, P.H., Y. Liu, R. L. McGraw, Y. Lee, J. Wang, G. Senum, M. Miller, and J.G. Hudson, 2008: Microphysical properties of stratus/stratocumulus clouds during the 2005 Marine Stratus/Stratocumulus Experiment (MASE). Submitted to *J. Geophys. Res.*

Gasparini, R., D.R. Collins, E. Andrews, P.J. Sheridan, J.A. Ogren, and J.G. Hudson (2006), Coupling aerosol size distributions and size-resolved hygroscopicity to predict humidity-dependent optical properties and CCN spectra, *J. Geophys. Res*., 111, D05S10, doi:10.1029/2005JD006092

Ghan, S.J. and S.E. Schwartz (2007), Aerosol properties and processes: A path from field and laboratory measurements to global climate models, *Bulletin, AMS* 88, 1059–1083, DOI: 10.1175/BAMS-88-7-1059

Hudson, J.G. (1989), An instantaneous CCN spectrometer, *J. Atmos. & Ocean. Techn., 6,* 1055-1065.

Hudson, J.G. (2007), Variability of the relationship between particle size and cloud-nucleating ability, *Geophys. Res. Let*., 34, L08801, doi:10.1029/2006GL028850.

Hudson, J.G. and D. J. Alofs (1981), Performance of the continuous flow diffusion chambers, *J. Rech. Atmos., 15,* 321-331.

Hudson, J.G. and X. Da (1996), Volatility and size of cloud condensation nuclei, *J. Geophys. Res.,* 101, 4435-4442.

Hudson, J.G. and P.R. Frisbie (1991), Cloud condensation nuclei near marine stratus*, J. of Geophys. Res.,* 96*,* D11, 20,795-20,808.

Hudson, J.G., and Y. Xie (1999), Vertical distributions of cloud condensation nuclei spectra over the summertime northeast Pacific and Atlantic Oceans, *J. Geophys. Res.* 104**,** 30219-30229.

Hudson, J.G., Y. Xie, and S.S. Yum (1998), Vertical distributions of cloud condensation nuclei spectra over the summertime Southern Ocean, *J. Geophys. Res.*, ***103,*** 16,609-16,624.

IPCC (2007), Climate Change 2007: The Physical Science Basis, Summary for Policymakers.1009 pp., Cambridge Univ. Press, New York.

Kocmond, W.C., C.F. Rogers, U. Katz, J.G. Hudson and J.E. Jiusto (1981), The 1980 International Cloud Condensation Nuclei Workshop, *Idojaras, 86,* No. 2-4, 160-168.

Yum, S.S., and J.G. Hudson (2001), Vertical distributions of cloud condensation nuclei spectra over the springtime Arctic Ocean, *J. Geophys. Res.,* 106, 15045-15052**.**

Twomey, S., and T.A. Wojciechowski (1969), Observations of the geographical variations of cloud nuclei, *J. Atmos. Sci*. 24, 702-702.

Below cloud concentrations

date	6	12	15	16	17	18	19	20	22	23	25	ave	ave(8)
CN	172	1318	840	658	1582	880	931	718	627	1096	971	**914**	893
1.0%	160	1039	448	475	720	795	829	588	506	819	609	**633**	614
0.60%	135	949	384	426	556	698	776	453	464	726	477	**562**	522
0.40%	102	811	311	375	411	566	666	378	398	637	359	**461**	427
0.30%	75	684	259	334	324	460	558	334	344	553	283	**384**	357
0.20%	45	499	193	277	231	324	404	278	269	432	199	**286**	268
0.15%	32	381	153	238	181	243	307	239	222	356	151	**225**	214
0.10%	21	243	102	184	126	155	199	188	163	265	98	**156**	149
0.08%	18	185	77	155	102	117	155	163	137	222	76	**125**	121
0.06%	14	123	50	118	78	79	111	135	107	173	52	**92**	90
0.04%	9		24	73	51	41	67	100	73	117	31	**57**	57

Table 1. Flight-averaged CN and CCN concentrations (number per cm^3) below cloud for all valid measured by the new CCN spectrometer. The last column is the average for the eight flights of July 15-22 and 25, the flights with low level polluted stratus.

Above cloud concentrations

date	6	12	15	16	17	18	19	20	22	23	25	ave	ave(8)
CN	256	428	1007	1130	1113	1391	1838	1208	634	690	1600	**1027**	1240
1.0%	108	248	751	1220	1082	1210	1818	1078	440	697	952	**873**	1069
0.60%	102	216	631	1178	946	976	1733	933	392	619	710	**767**	938
0.40%	96	186	497	1107	783	741	1515	760	342	549	502	**644**	781
0.30%	89	164	395	1024	654	578	1273	622	298	480	373	**541**	652
0.20%	77	131	261	861	481	380	889	440	236	383	237	**398**	473
0.15%	69	108	185	720	372	270	644	331	190	323	167	**307**	360
0.10%	56	77	102	509	252	157	377	212	136	249	103	**203**	231
0.08%	49	61	72	399	200	113	272	164	109	213	77	**157**	176
0.06%	41	41	43	277	145	71	175	115	80	170	51	**110**	120
0.04%	29		19	150	91	36	91	69	52	118	29	**68**	67

Table 2. As Table 1 but just above cloud.

date	6	12	15	16	17	18	19	20	22	23	25	ave	av(8)
CN	1.49	0.32	1.20	1.72	0.70	1.58	1.97	1.68	1.01	0.63	1.65	1.12	1.39
1.0%	0.68	0.24	1.68	2.57	1.50	1.52	2.19	1.83	0.87	0.85	1.56	1.38	1.74
0.60%	0.76	0.23	1.64	2.77	1.70	1.40	2.23	2.06	0.84	0.85	1.49	1.36	1.80
0.40%	0.94	0.23	1.60	2.95	1.91	1.31	2.27	2.01	0.86	0.86	1.40	1.40	1.83
0.30%	1.19	0.24	1.53	3.07	2.02	1.26	2.28	1.86	0.87	0.87	1.32	1.41	1.83
0.20%	1.71	0.26	1.35	3.11	2.08	1.17	2.20	1.58	0.88	0.89	1.19	1.39	1.76
0.15%	2.16	0.28	1.21	3.03	2.06	1.11	2.10	1.38	0.86	0.91	1.11	1.36	1.68
0.10%	2.67	0.32	1.00	2.77	2.00	1.01	1.89	1.13	0.83	0.94	1.05	1.30	1.55
0.08%	2.72	0.33	0.94	2.57	1.96	0.97	1.75	1.01	0.80	0.96	1.01	1.26	1.45
0.06%	2.93	0.33	0.86	2.35	1.86	0.90	1.58	0.85	0.75	0.98	0.98	1.20	1.33
0.04%	3.22		0.79	2.05	1.78	0.88	1.36	0.69	0.71	1.01	0.94	1.19	1.18
ave	1.86	0.28	1.25	2.63	1.78	1.19	1.98	1.46	0.84	0.89	1.25	1.31	1.59

Table 3. Ratio of just above cloud to just below cloud concentrations for CN and CCN at various cumulative S values (Table 2/Table 1).

date	6	12	15	16	17	18	19	20	22	23	25	ave
CN	0.52	0.03	0.37	0.41	0.50	0.17	1.23	0.12	0.12	2.22	0.50	**0.56**
1%	0.45	0.23	0.12	0.37	0.30	0.15	1.09	0.20	0.16	0.49	0.56	**0.38**
0.6%	0.42	0.27	0.12	0.35	0.29	0.15	0.98	0.22	0.18	0.49	0.48	**0.36**
0.4%	0.38	0.33	0.14	0.32	0.29	0.15	0.80	0.24	0.21	0.46	0.42	**0.34**
0.3%	0.36	0.39	0.17	0.29	0.29	0.15	0.67	0.25	0.23	0.43	0.37	**0.33**
0.2%	0.51	0.47	0.22	0.25	0.31	0.17	0.54	0.26	0.25	0.37	0.36	**0.34**
0.15%	0.72	0.49	0.26	0.24	0.32	0.18	0.47	0.28	0.27	0.31	0.41	**0.36**
0.1%	1.01	0.48	0.32	0.25	0.35	0.20	0.43	0.29	0.30	0.24	0.58	**0.40**
0.08%	1.15	0.46	0.36	0.26	0.37	0.23	0.43	0.30	0.32	0.22	0.70	**0.44**
0.06%	1.30	0.43	0.41	0.29	0.39	0.26	0.45	0.32	0.34	0.21	0.91	**0.48**
0.04%	1.50		0.50	0.34	0.44	0.34	0.51	0.34	0.39	0.22	1.22	**0.58**
ave	**0.76**	**0.36**	**0.27**	**0.31**	**0.35**	**0.20**	**0.69**	**0.26**	**0.25**	**0.51**	**0.59**	**0.42**

Table 4. Relative variability of the below cloud concentrations expressed by the standard deviation divided by the mean concentrations (Table 1).

date	simultan-eous time below	new time below	simul/ new below	total new time below	new/ total below	simultan-eous time above	new time above	simul/ new above	total new above	new/ total above
6	559	948	0.59	4262	0.22	364	525	0.69	560	0.94
12	119	535	0.22	535	1.00	353	353	1.00	712	0.50
15	748	836	0.90	4908	0.17	20	74	0.27	857	0.09
16	210	723	0.29	6610	0.11	138	455	0.30	1660	0.27
17	851	1800	0.47	6650	0.27	124	188	0.66	2455	0.08
18	1236	1236	1.00	4625	0.27	52	371	0.14	749	0.50
19	135	995	0.14	1213	0.82	151	299	0.50	6539	0.05
20	396	396	1.00	2554	0.15	122	423	0.29	6764	0.06
22	497	710	0.70	1346	0.53	39	122	0.32	7345	0.02
23	*931	1209	0.77	3833	0.31	22	206	0.11	3387	0.06
25	*289	289	1.00	422	0.61	46	207	0.22	3127	0.07
total	5971	9677		36958		1431	3223		34155	
ave	543	880	0.64	3360	0.41	130	293	0.41	3105	0.24
sd	362	431	0.33	2288	0.30	123	145	0.27	2618	0.29

* These numbers do not match those in Fig. 5s, u, w and x because they are the sum of the low and high concentration measurements.

Table 5. Columns 1and 6 show number of seconds of valid simultaneous measurements by both CCN spectrometers below and just above cloud respectively for each flight. Columns 2 and 7 show the total number of seconds of valid measurements by the new spectrometer. Columns 3 and 8 show ratios of the previous two Measurement times (s) columns—the fraction of time of simultaneous measurements to total new spectrometer measurement times. Columns 4 and 9 show total elapsed time over which the new spectrometer made valid measurements for each flight. Columns 5 and 10 show the fraction of time that the new spectrometer was making valid measurements out of the total elapsed time over which those measurements were made (column 2/column 4 and column 7/column 9, respectively).

Consistent concentrations

	23 July 10:22:01-10:22:46				18 July 11:05:00-11:05:20				25 July 12:14:10-12:14:30			
	ave	sd	sd/ ave	[sd/ave]/ $[(cts)^{.5}/cts]$	ave	sd	sd/ ave	[sd/ave]/ $[(cts)^{.5}/cts]$	ave	sd	sd/ ave	[sd/ave]/ $[(cts)^{.5}/cts]$
CN	660	7.0	0.011	1.12	1548	9.8	0.006	1.02	710	5.0	0.007	0.77
1.0%	550	46.4	0.084	1.14	1390	54.8	0.039	0.85	345	35.4	0.103	1.10
0.60%	486	43.0	0.088	1.13	1166	59.3	0.051	1.00	304	32.4	0.107	1.08
0.40%	433	39.1	0.090	1.09	922	61.0	0.066	1.16	247	32.4	0.131	1.19
0.30%	386	37.9	0.098	1.11	743	55.6	0.075	1.18	210	29.6	0.141	1.18
0.20%	319	33.7	0.106	1.09	511	50.8	0.099	1.30	160	23.3	0.145	1.06
0.15%	275	28.3	0.103	0.99	373	39.7	0.106	1.19	129	24.0	0.186	1.22
0.10%	214	27.7	0.129	1.09	224	29.8	0.133	1.15	88	23.0	0.261	1.41
0.08%	184	26.4	0.143	1.12	165	25.9	0.158	1.17	68	19.9	0.295	1.40
0.06%	147	26.5	0.180	1.26	111	22.3	0.201	1.22	46	14.9	0.324	1.27
0.04%	99	20.7	0.209	1.20	58	19.5	0.336	1.48	26	10.7	0.420	1.23

Table 6. Mean concentrations during flight legs when they were so consistent that the relative standard deviation were similar to the limitations of both instruments to detect variations, i.e., the square root of the actual number of pulses counted to the average number of pulses counted within each 1 s record. The first example 23 July is shown in Fig. 7b. There was similar variability over the entire period shown in Fig. 7b, which is a total distance of 9 km (aircraft speed 100 m/s). The 23 July and 25 July examples were below cloud but the 18 July example was just above cloud.

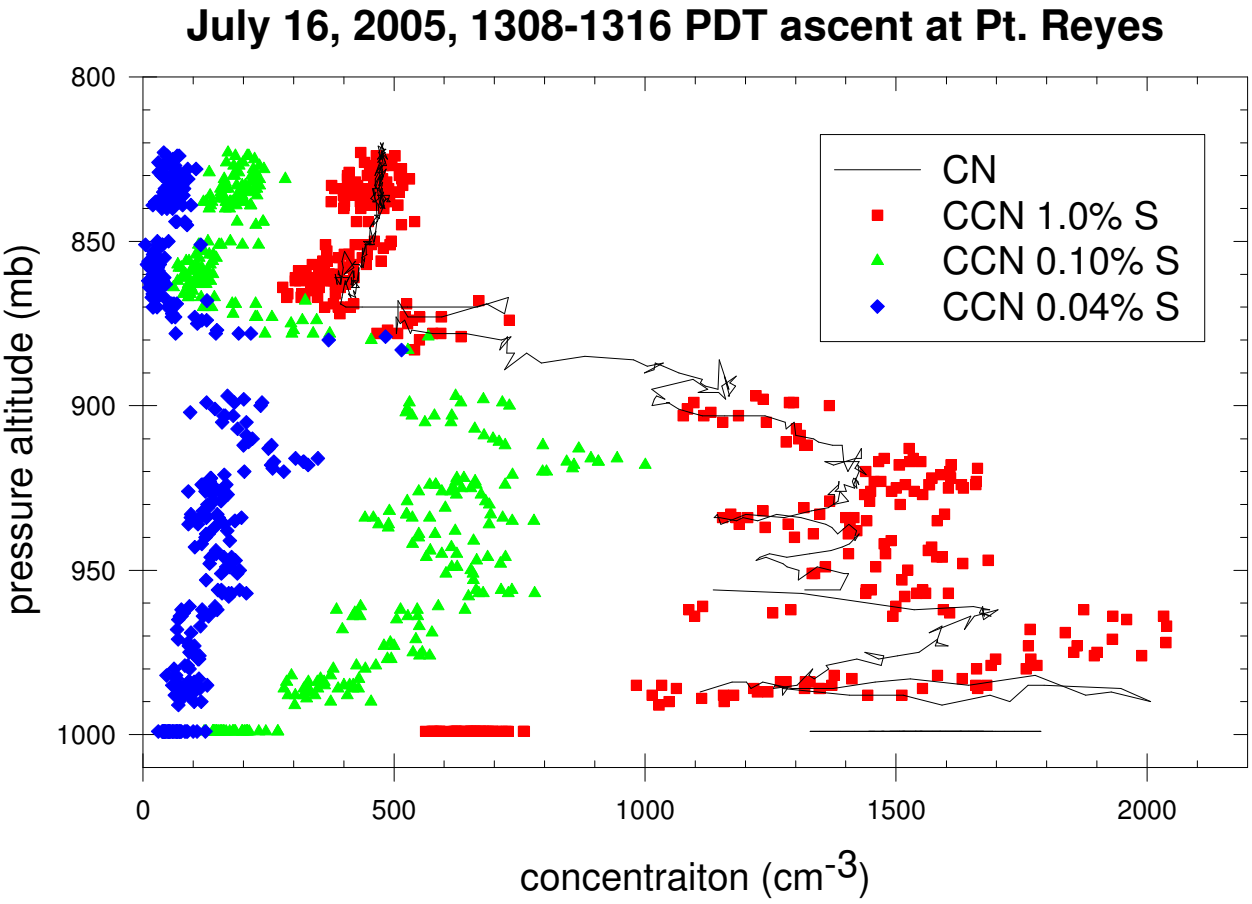

Figure 1. Continuous measurement of the vertical profile of CN and CCN at Pt. Reyes at the coast 80 km north of San Francisco.

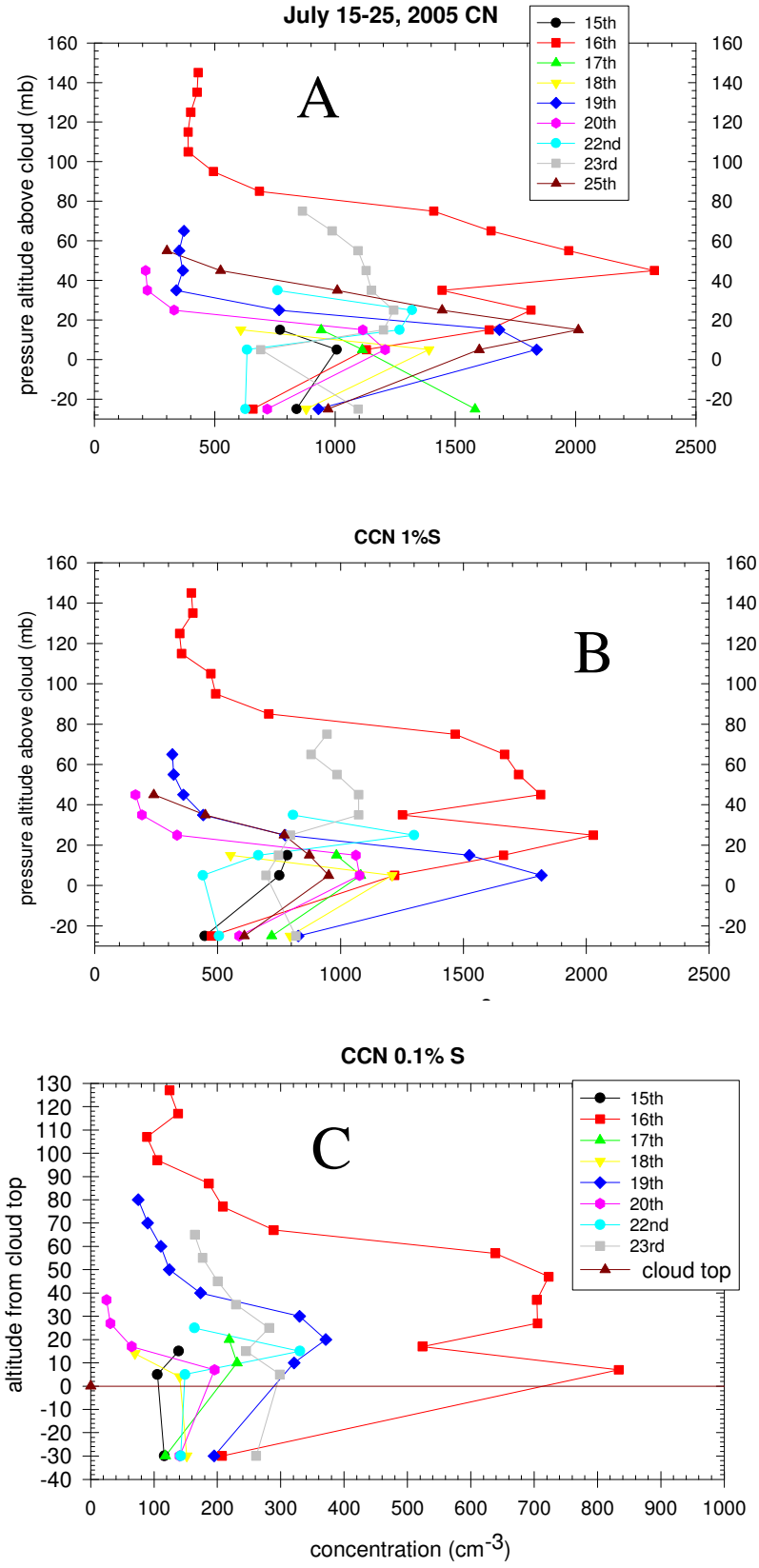

Figure 2. Pressure altitude 10 mb bin-averaged concentrations of CN and CCN @ 1% S and 0.4% S. Altitudes are normalized to average cloud top for each flight (0 mb). All below cloud (near surface) measurements are arbitrarily set to –25 mb.

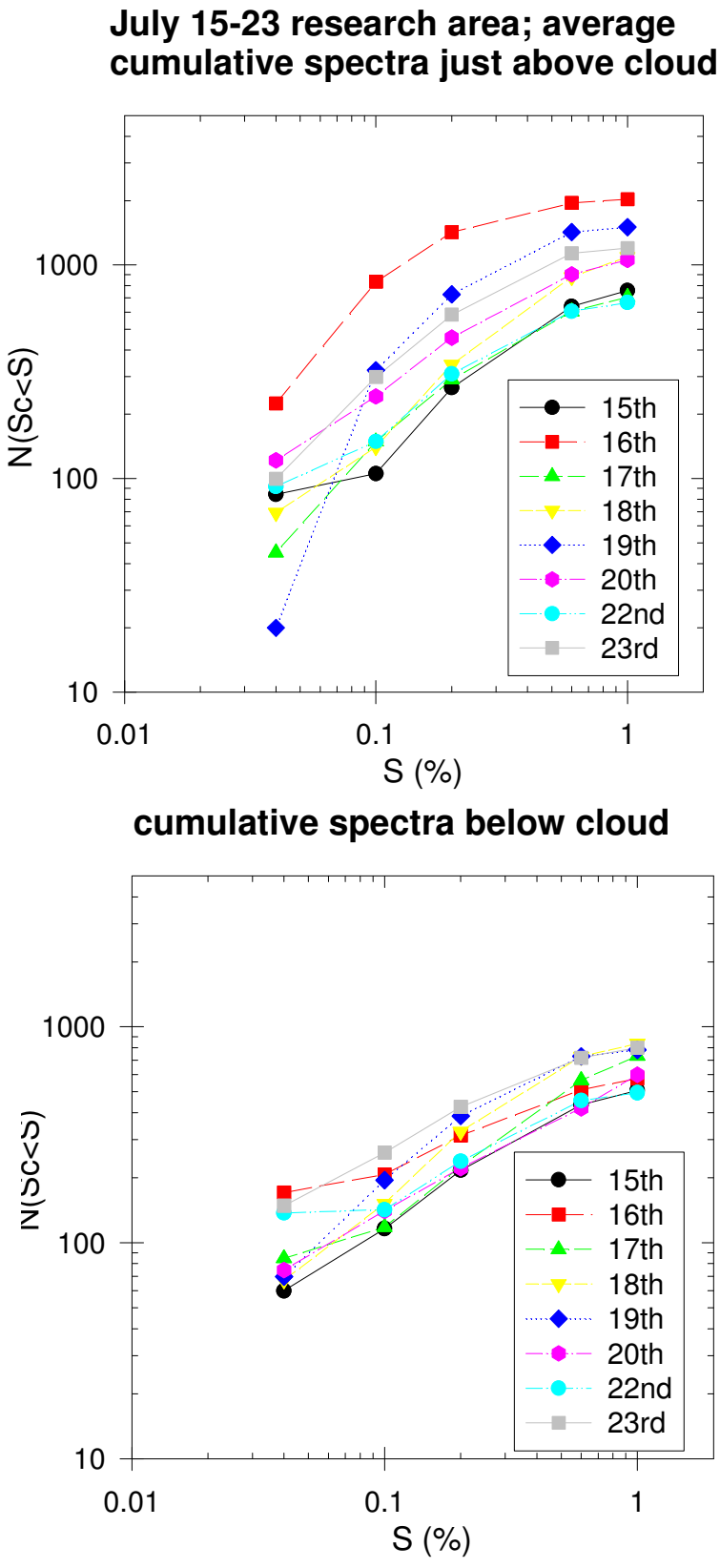

Figure 3. Average cumulative spectra for each flight above and below cloud.

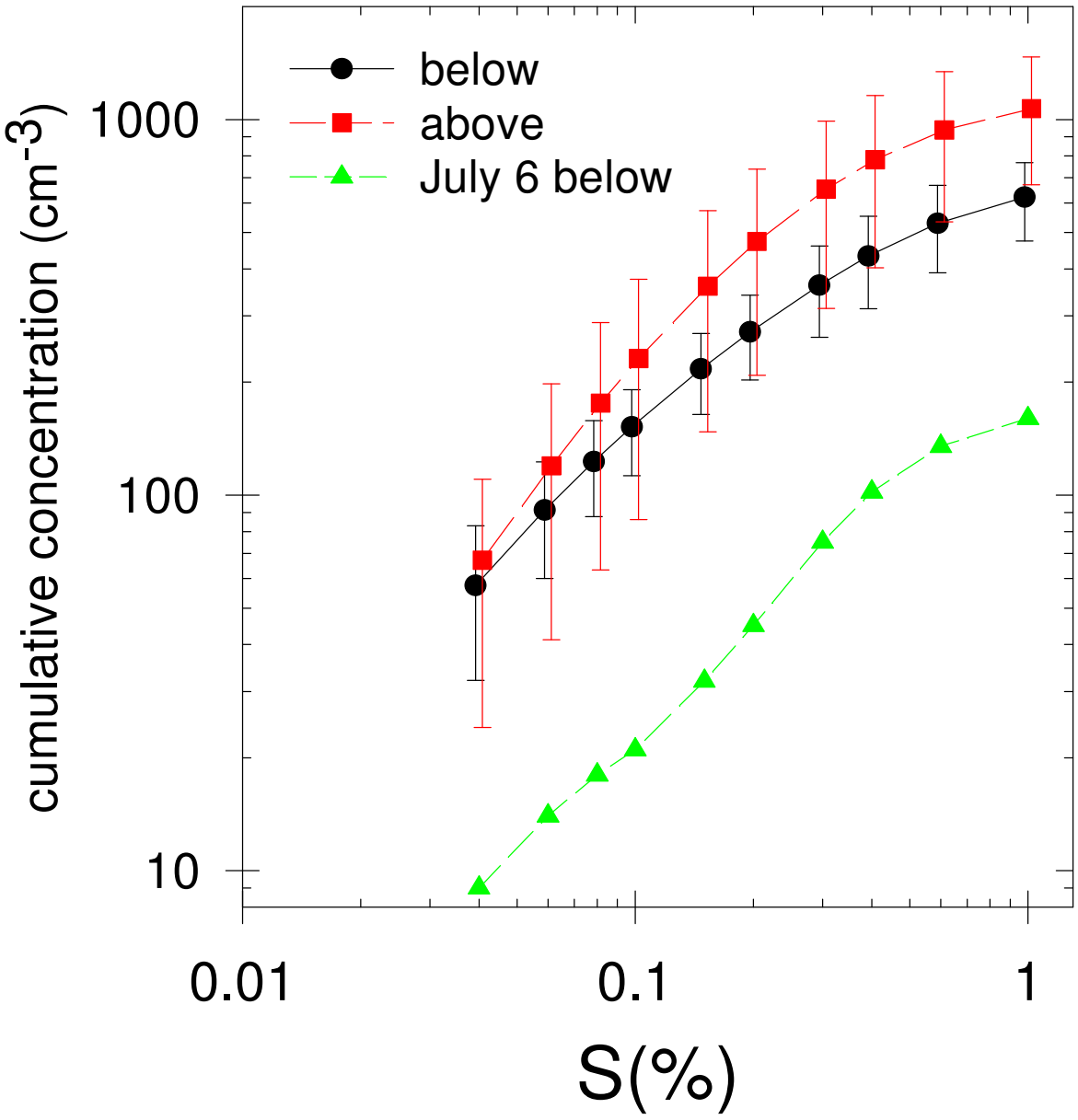

Figure 4. Average CCN spectra below and above cloud for the 8 flights with unbroken polluted stratus—July 15, 16, 17, 18, 19, 20, 22, and 25 and the one maritime flight of July 6.

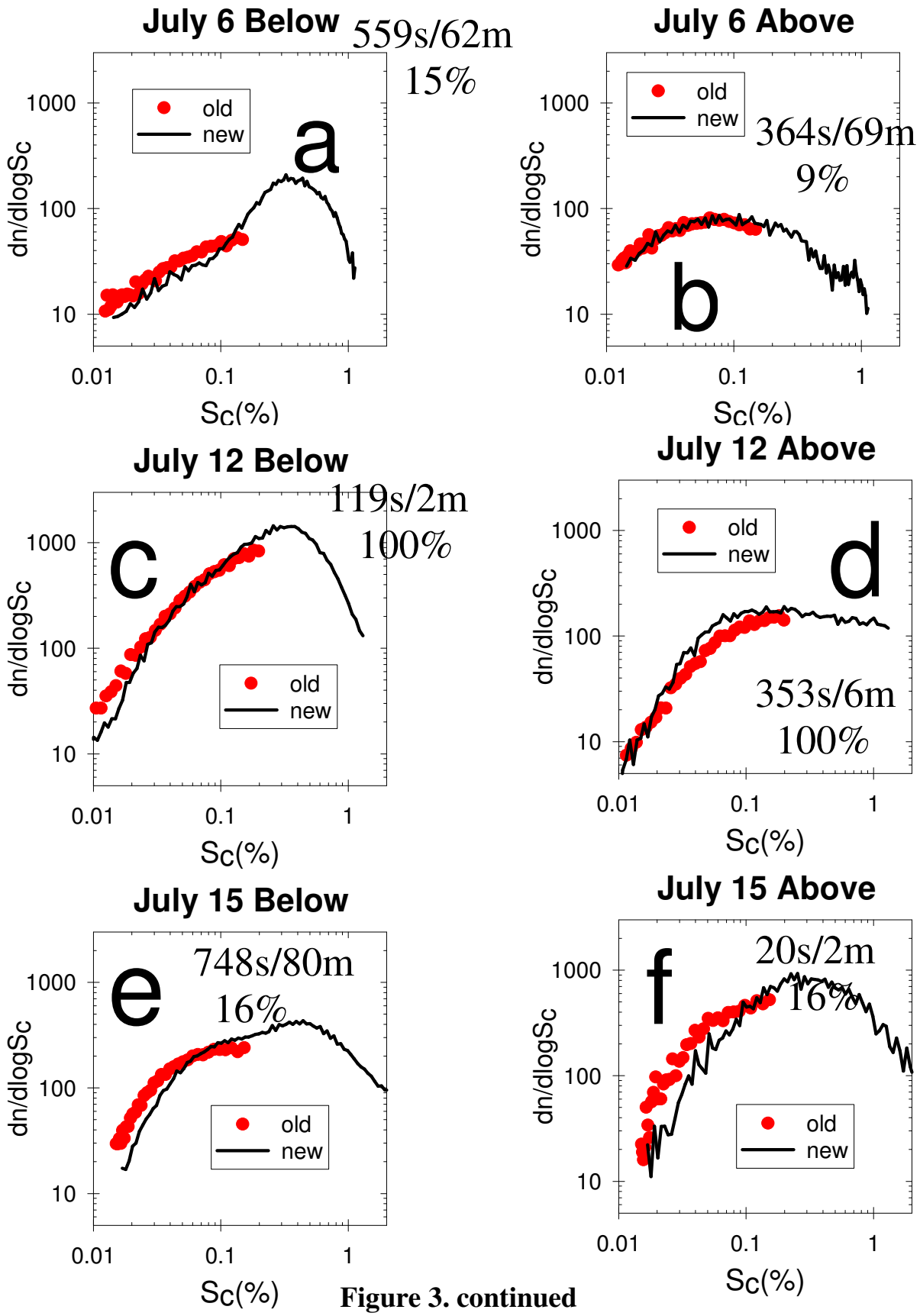

Figure 3. continued

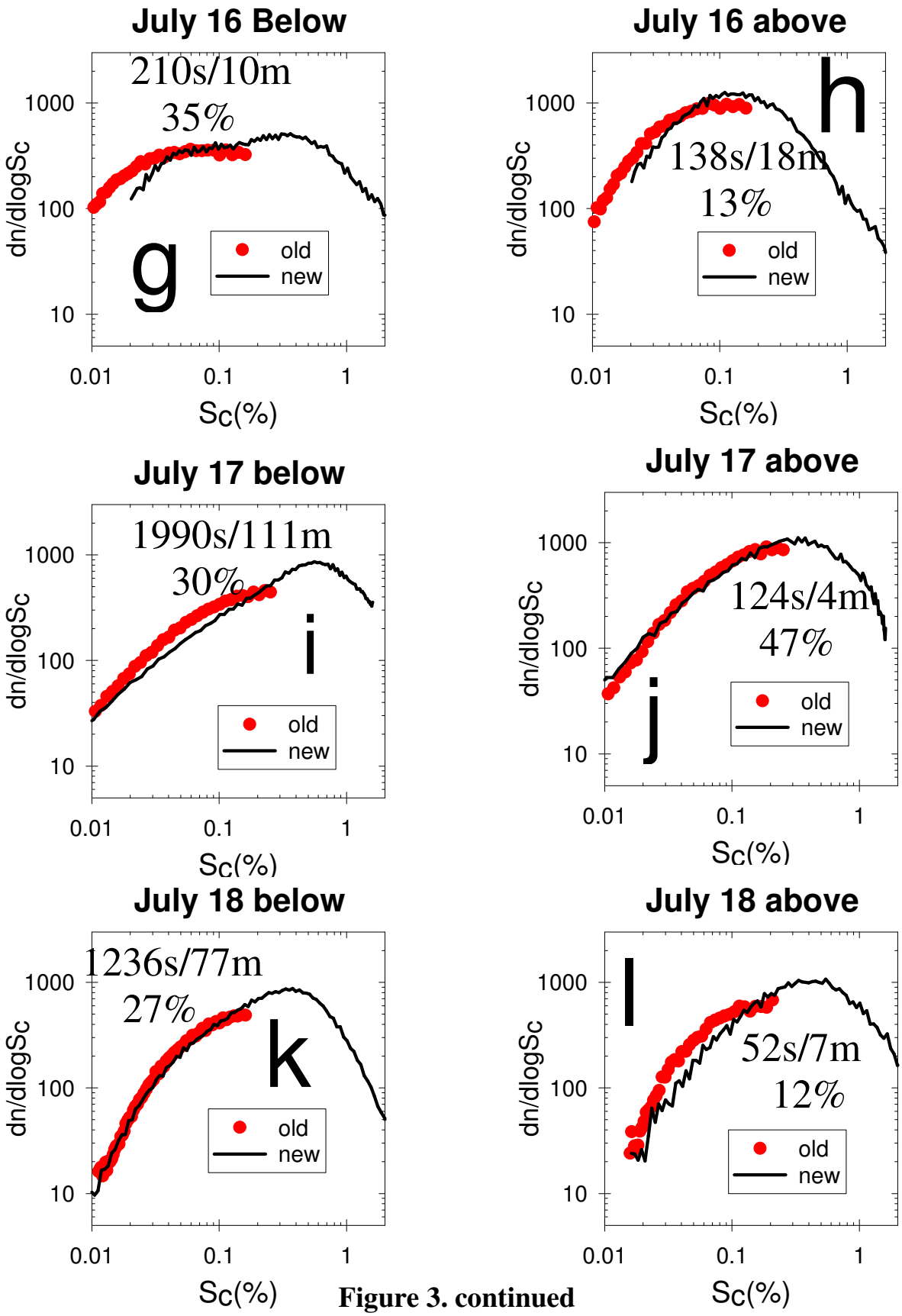

Figure 3. continued

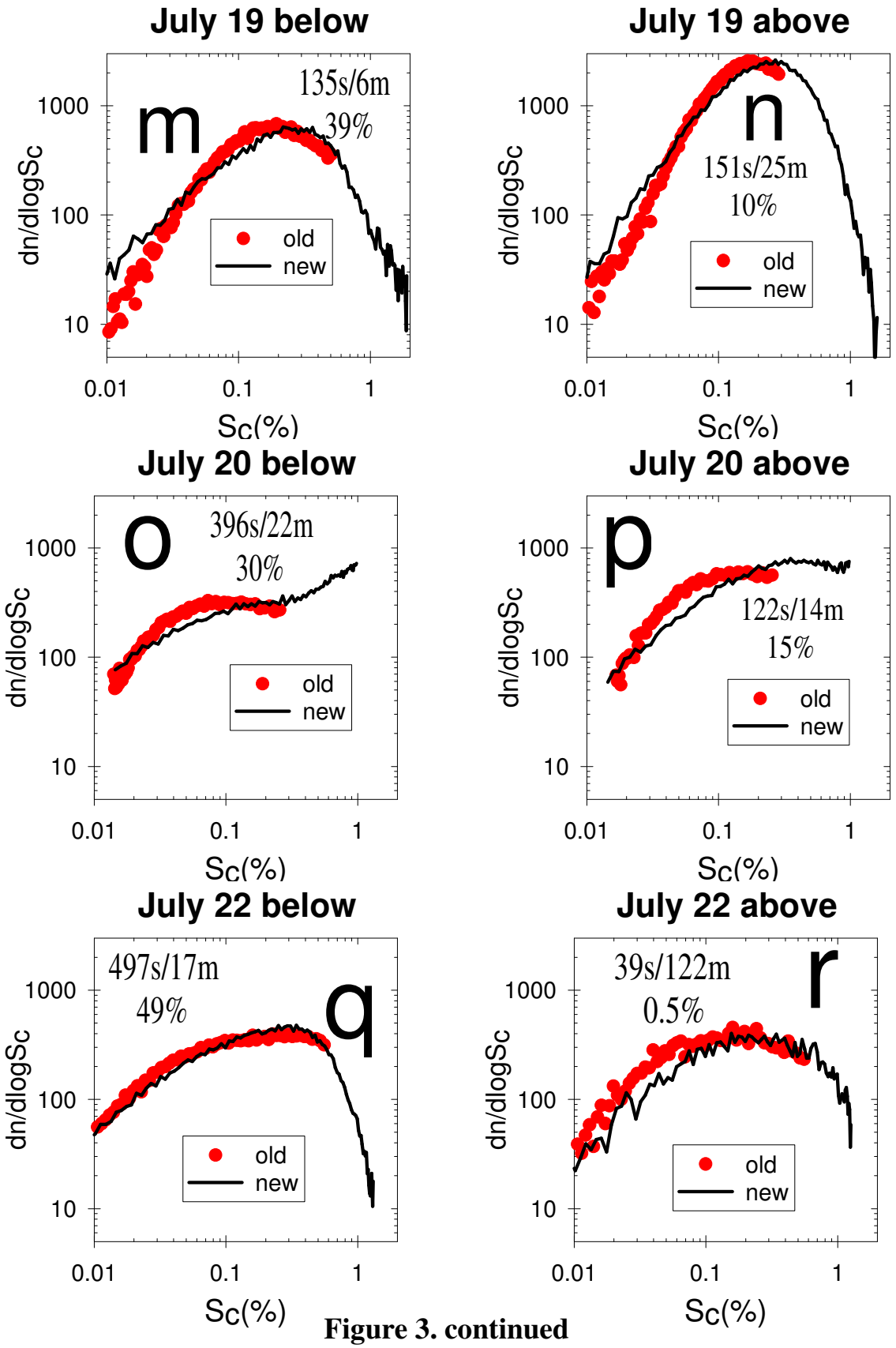

Figure 3. continued

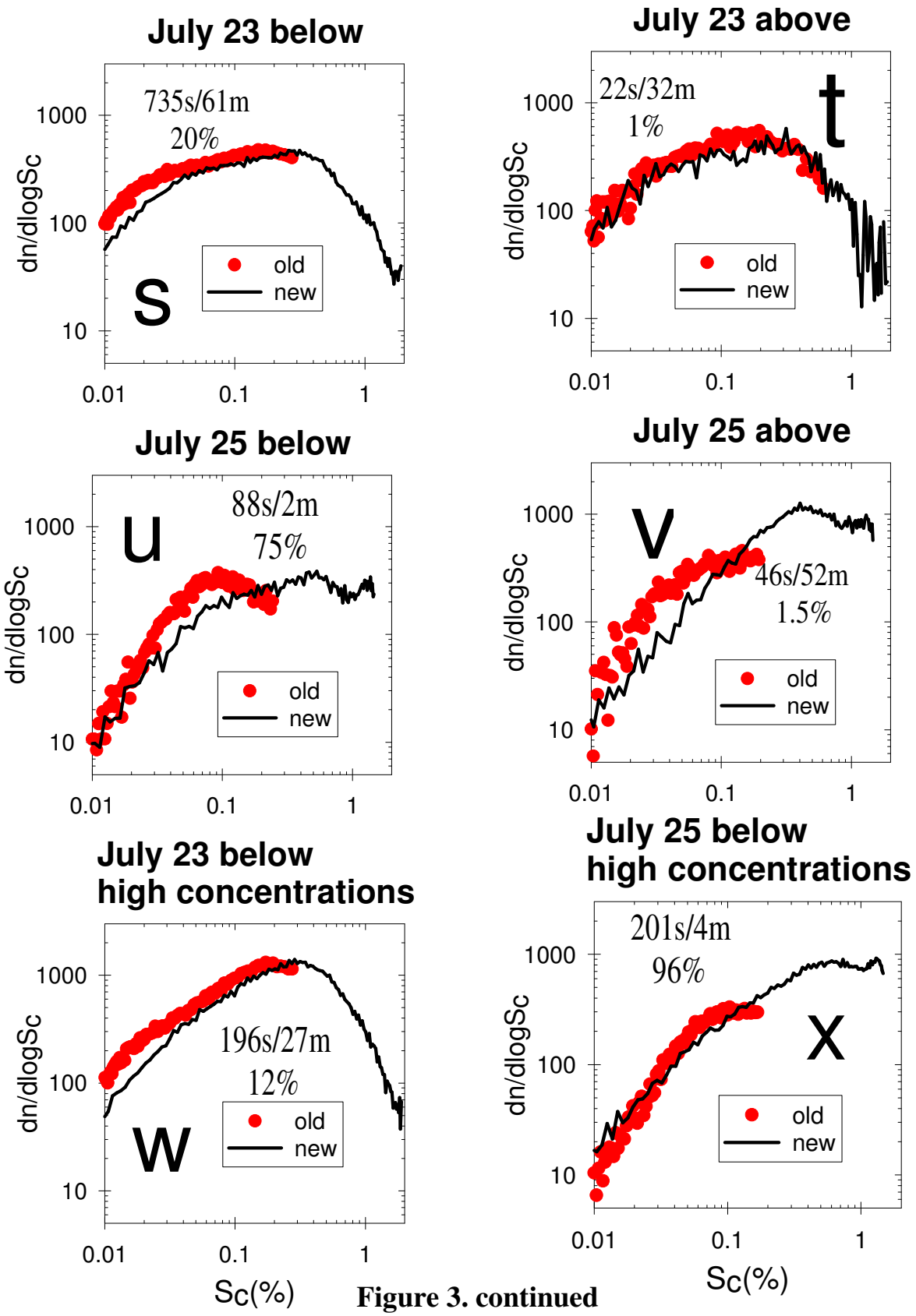

Figure 3. continued

Figure 5. Differential CCN spectra for all valid below (left panels) and above (right panels) cloud measurements of each flight when there was simultaneous data from both CCN spectrometers. In each panel are shown the total time in seconds of the measurements and the total elapsed time (rounded to the nearest minute) over which these measurements were obtained. The percentage below these numbers is their dividend. Data from the last two flights was divided according to concentration.

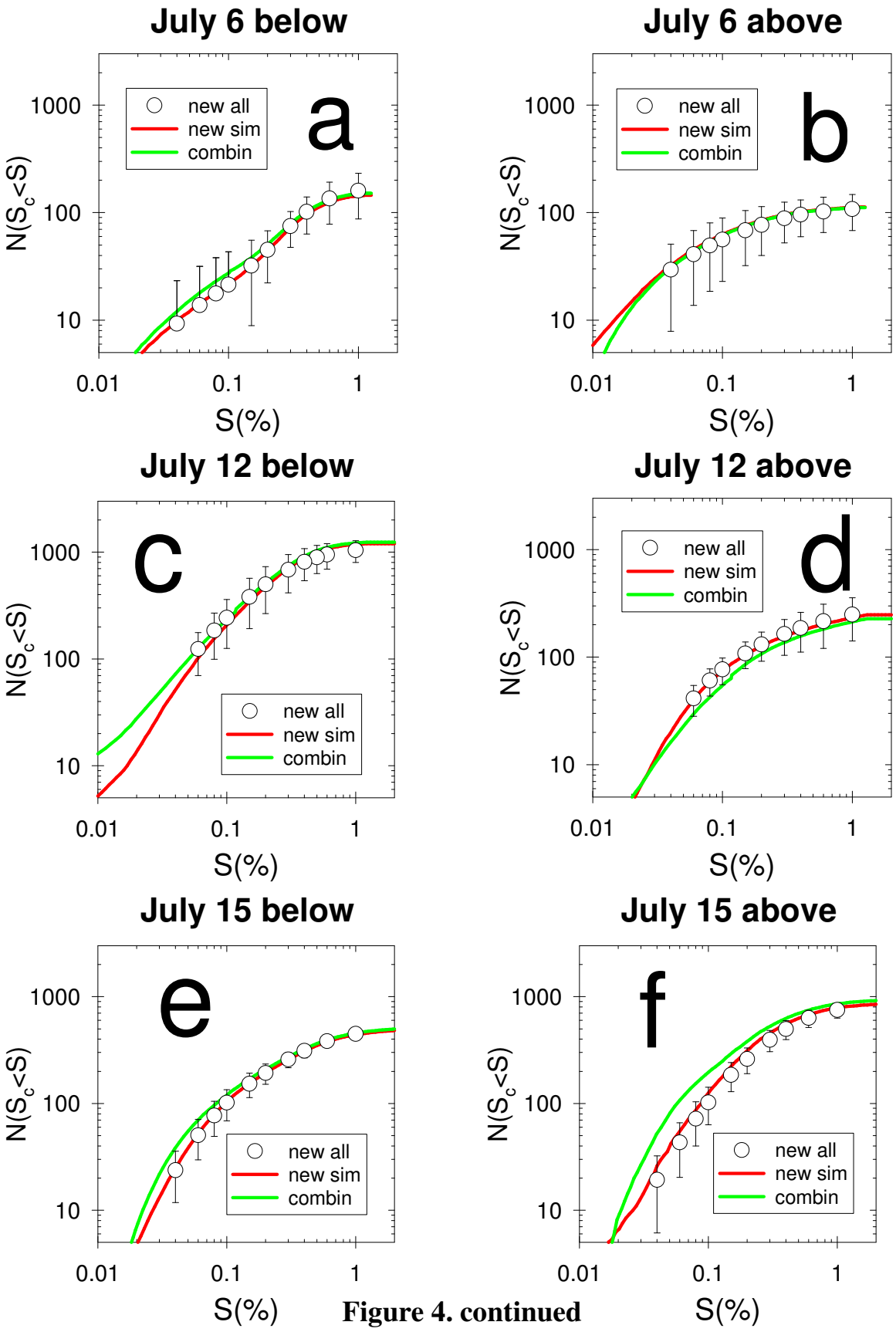

Figure 4. continued

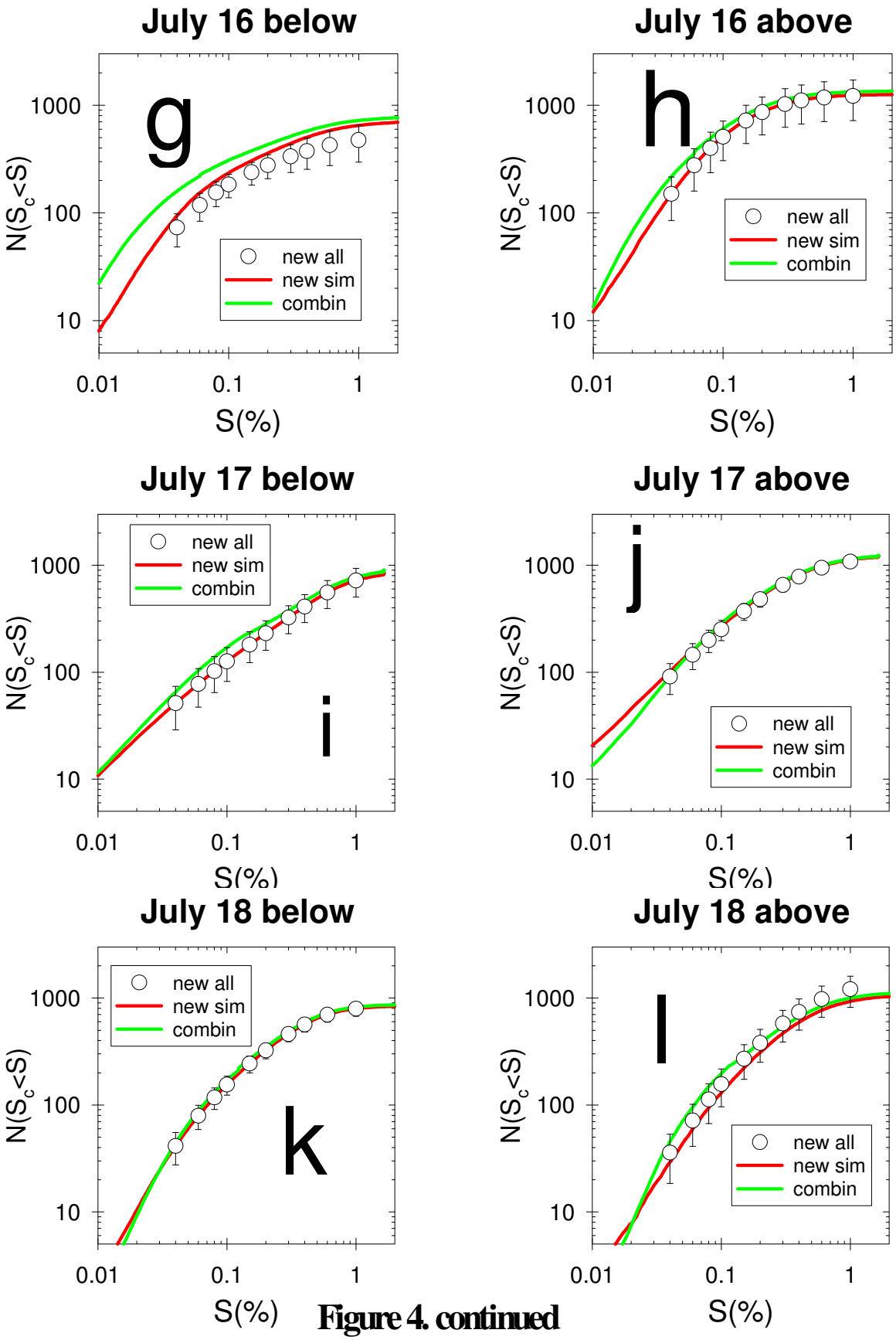

Figure 4. continued

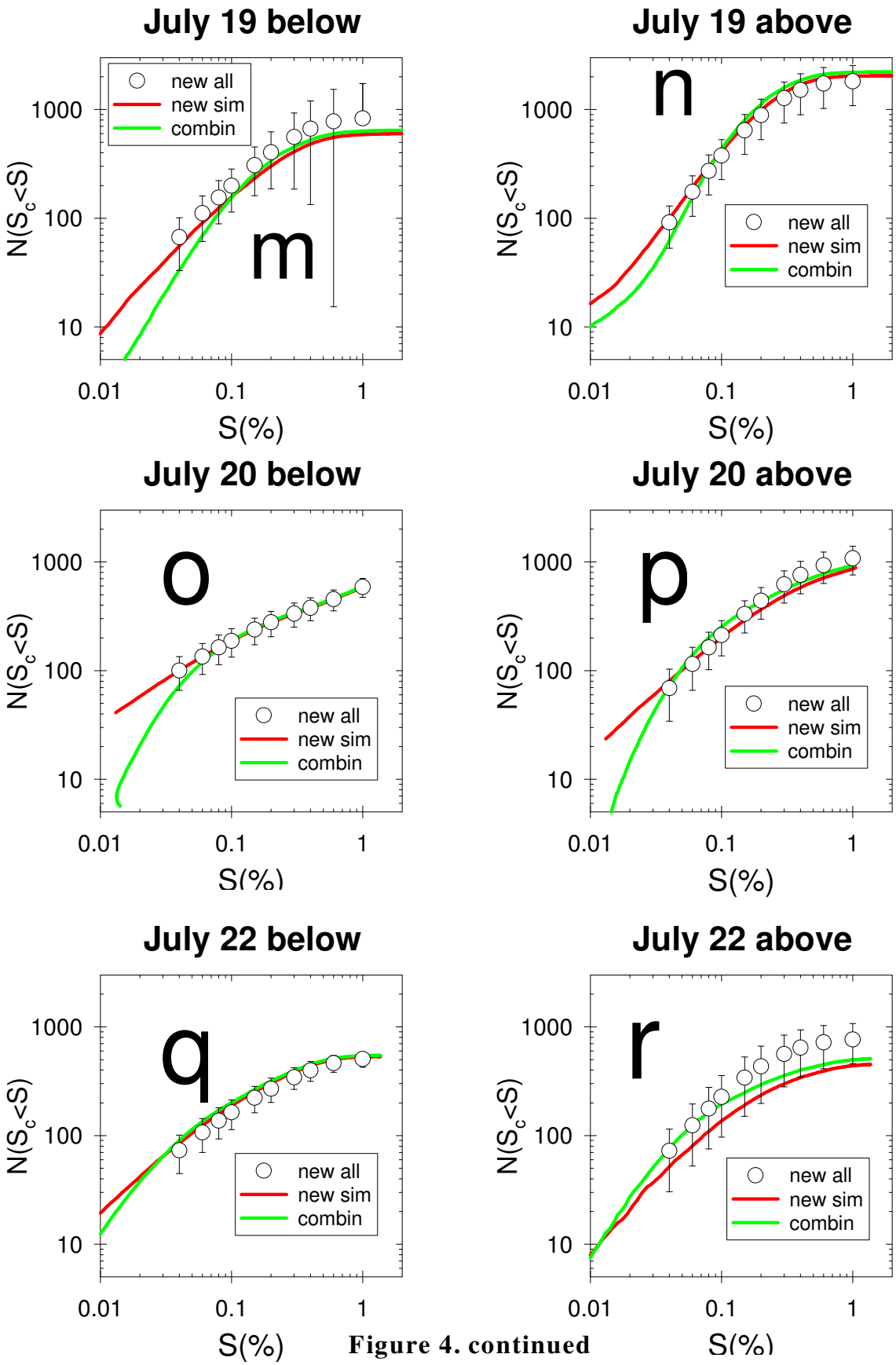

Figure 4. continued

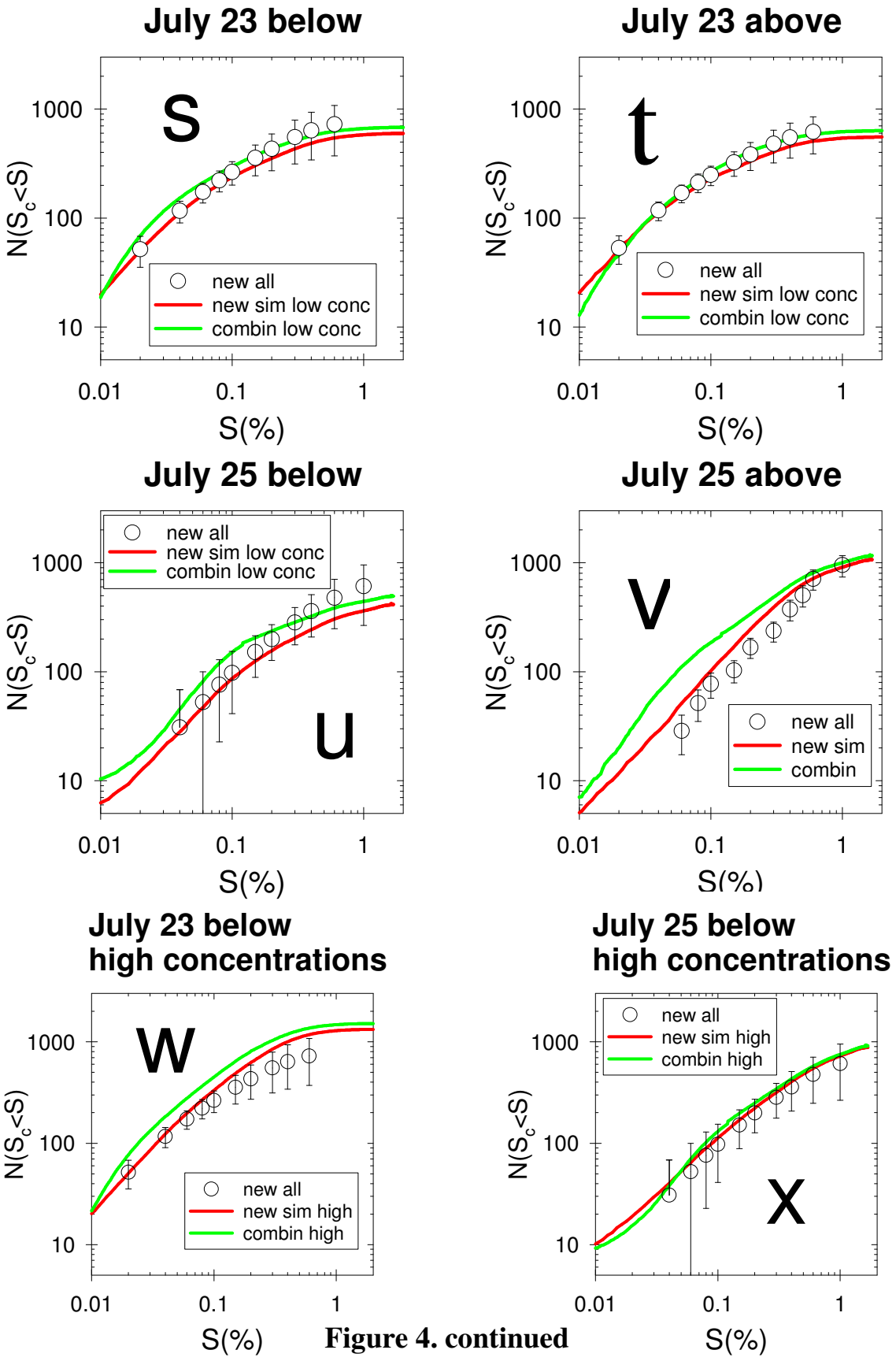

Figure 4. continued

Figure 6. Similar to Fig. 5 except cumulative plots. The red line is the same data in Fig. 5 for the new spectrometer (black line in Fig. 5). The green line is the composite data from both spectrometers. So at low S it is the same as Fig. 5 for the old spectrometer (red line). The open circles are the new spectrometer data for the entire period, which thus includes time periods when the old spectrometer was not obtaining valid simultaneous data. The error bars are the standard deviations of these data, which are integrations over 1 s time periods.

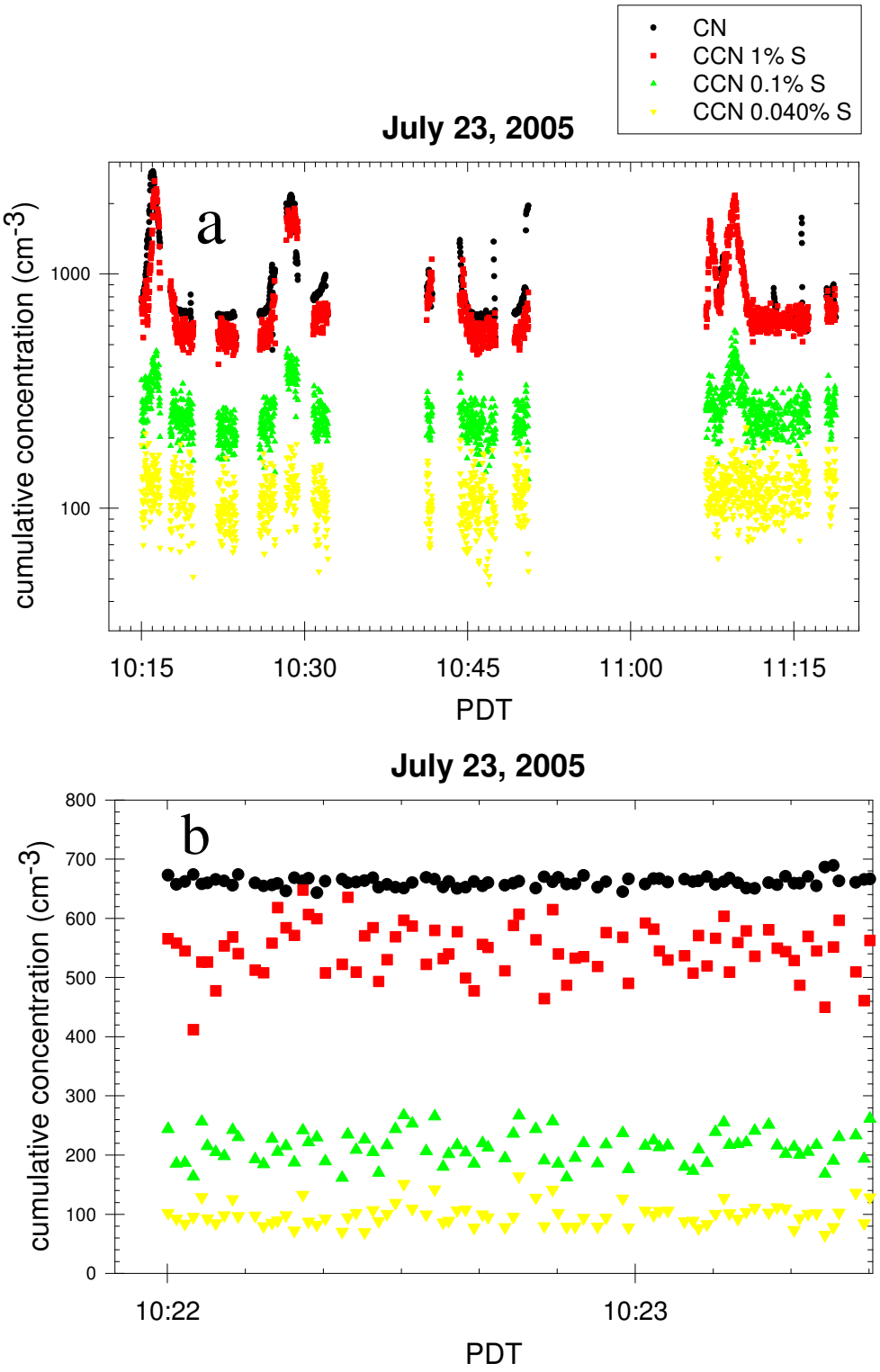

Figure 7. Time plot of valid ambient CN and CCN concentrations below cloud during a) the entire middle part of the flight, b) when the concentrations were very steady.

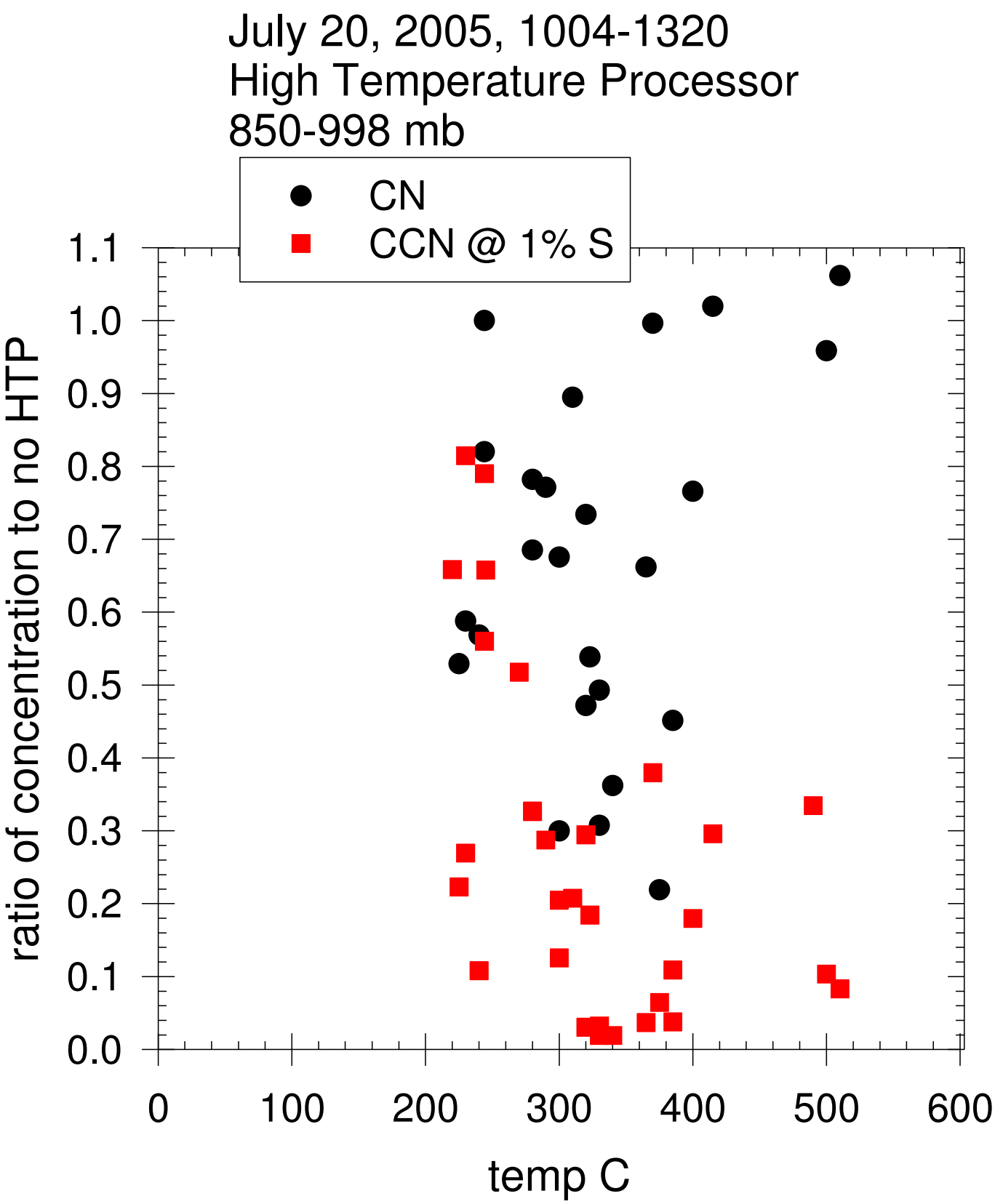

Figure 8. Volatility measurement.

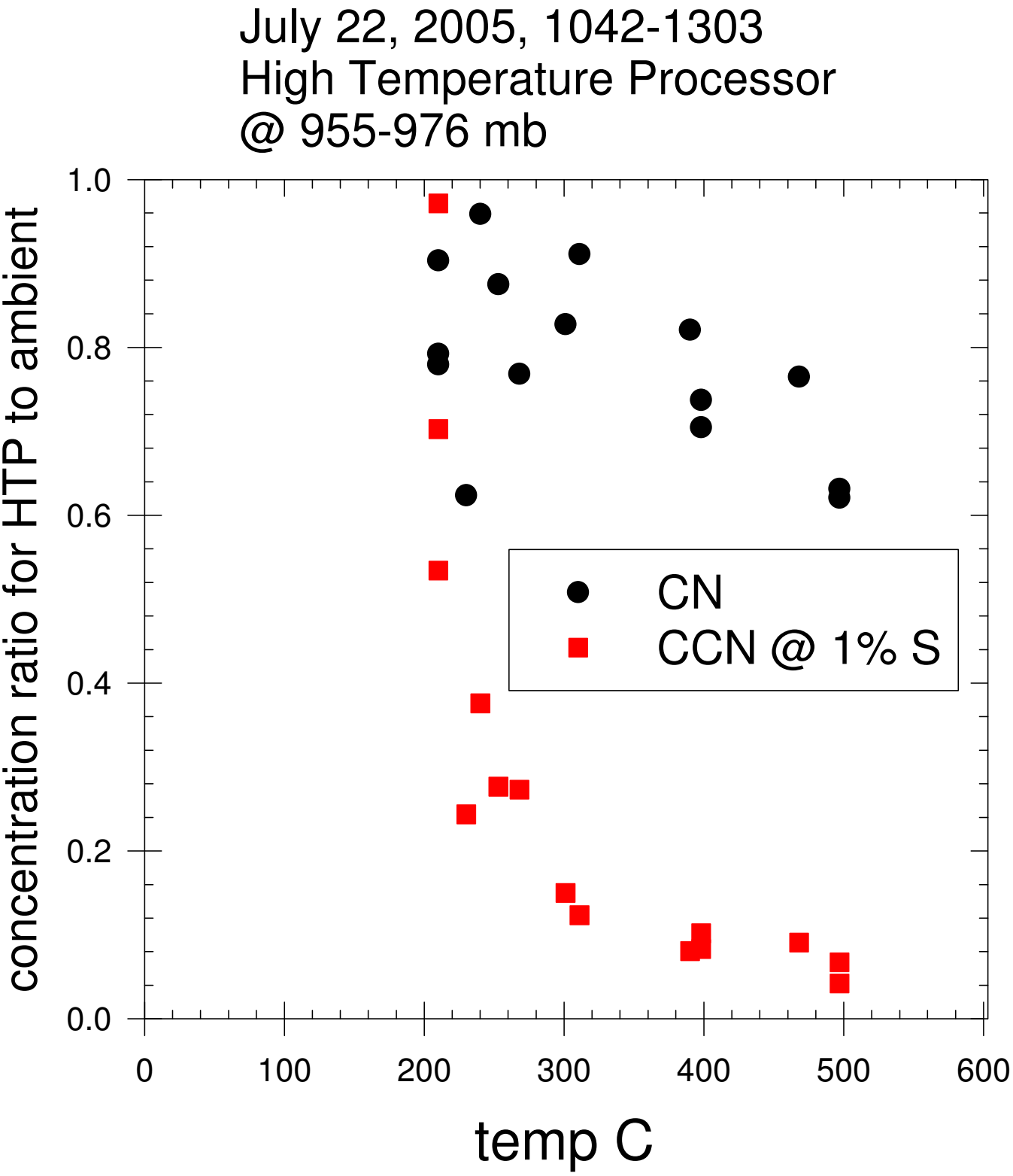

Figure 9. Volatility measurement.

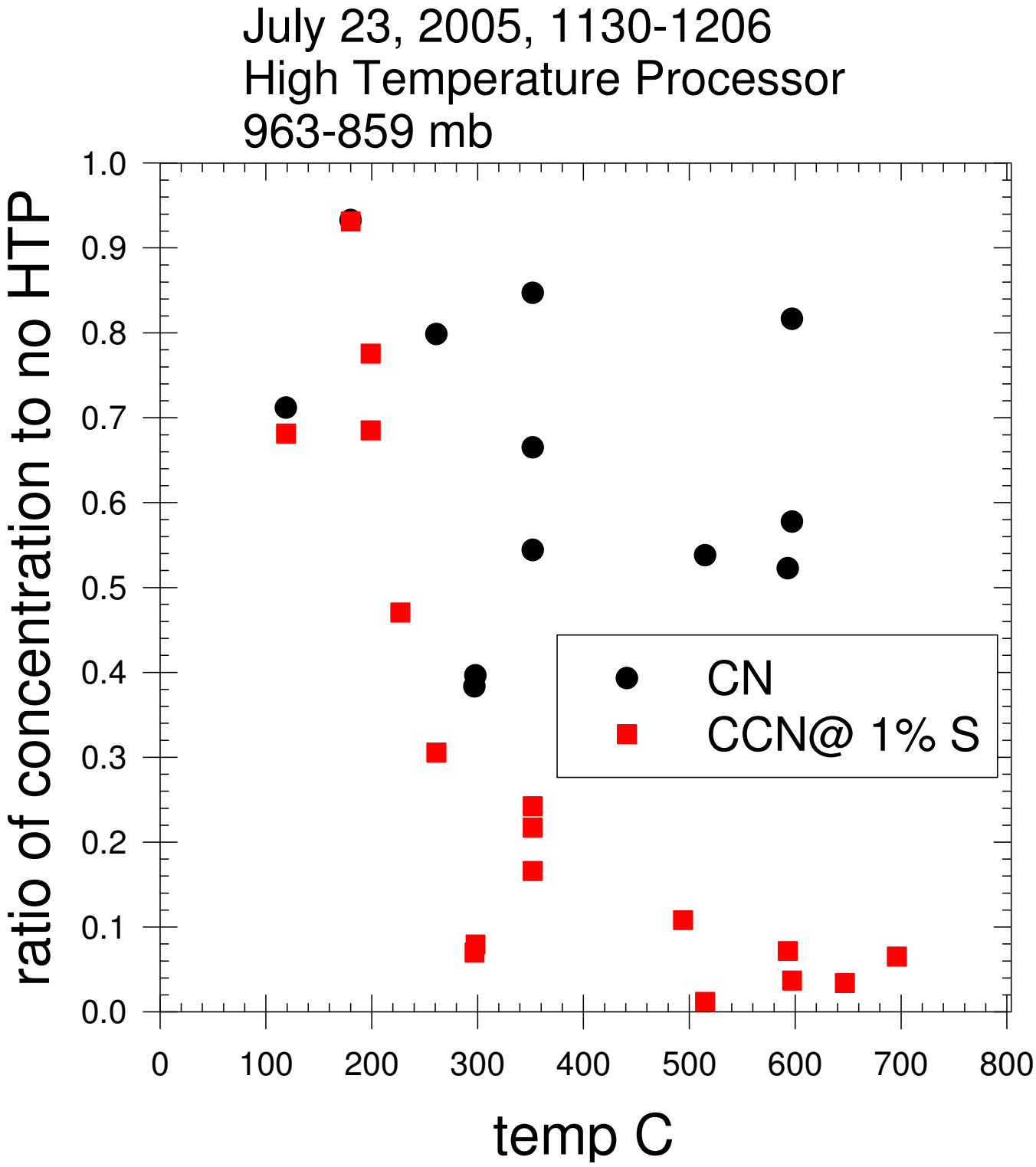

Figure 10. Volatility measurement.

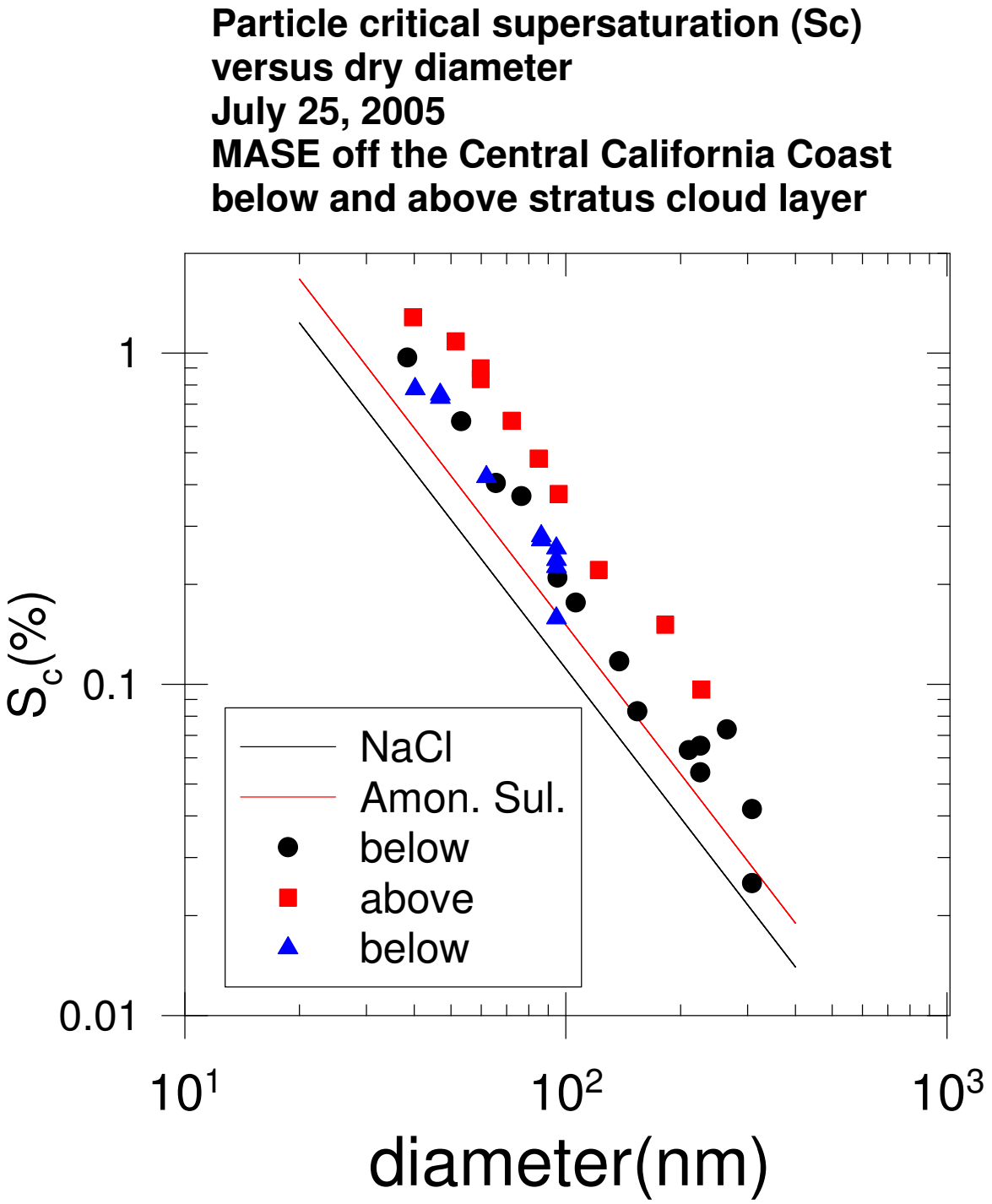

Figure 11. Dry particle size versus critical supersaturation (S_c) data and theoretical lines for two soluble substances..

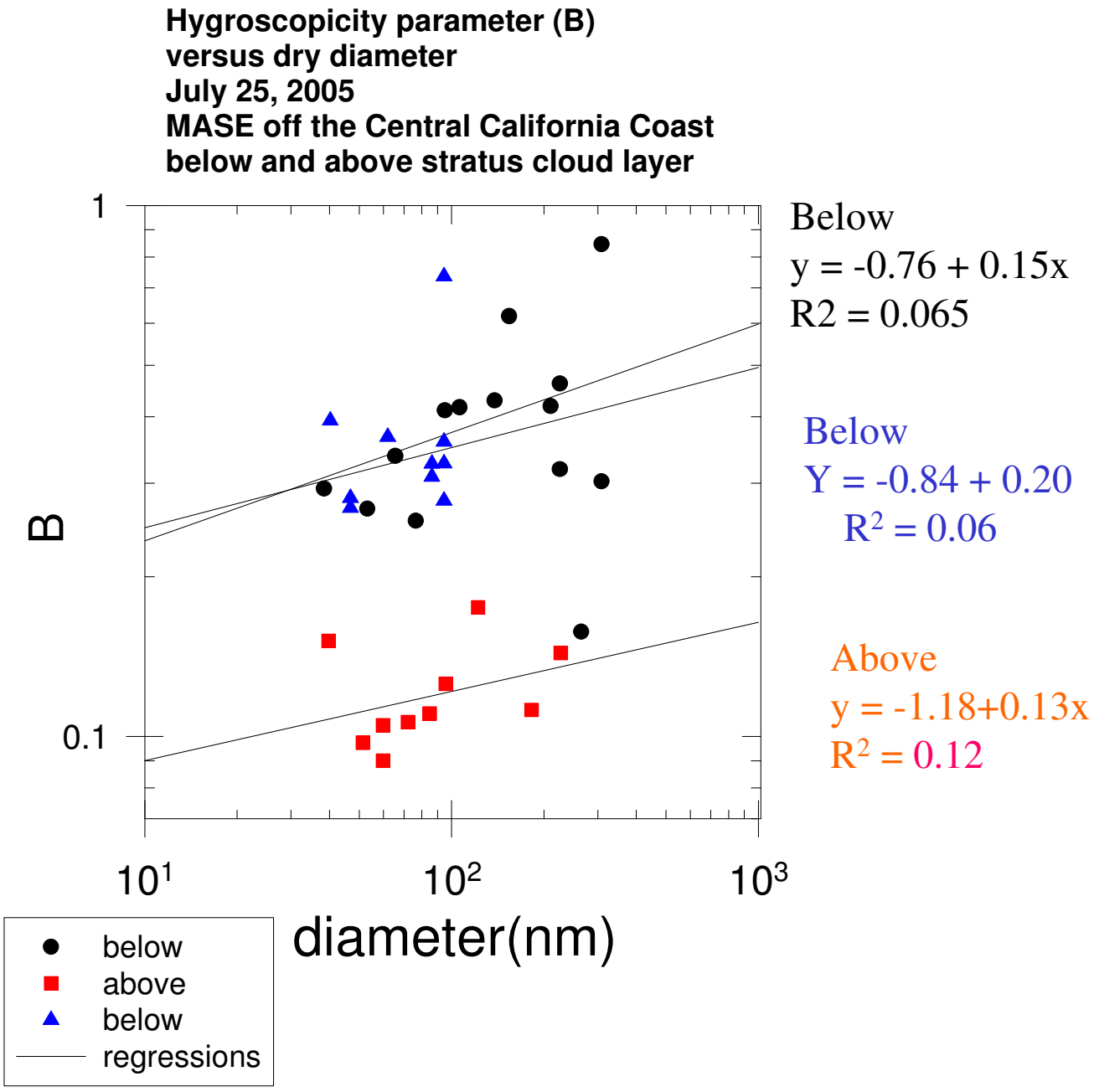

Figure 12. Hygroscopicity (B) or solubility versus dry particle diameter for the data in Fig. 11. The linear regression equations are shown.